Journal of Industrial and Management Optimization

https://www.aimspress.com/journal/jimo

JIMO, 22(12): 6399–6441.
DOI:10.3934/jimo.2026215
Received: 15 July 2026
Revised: 12 October 2026
Accepted: 28 October 2026
Published: 11 November 2026

Research article

A dynamic low-carbon supply chain coordination model under cap-and-trade regulation and the retailer's disadvantageous inequity aversion

Bo Xu and Yunlong Tian*

Business School, University of Shanghai for Science and Technology, No. 334 Jungong Road, Yangpu District, Shanghai 200093, China

* **Correspondence:** Email: 254491186@st.usst.edu.cn.

Abstract: In this paper, we examined how carbon pricing and retailer inequity aversion interact through profit allocation in a two-echelon low-carbon supply chain. The analysis distinguished behavioral responses from material-profit outcomes. A finite-horizon open-loop model combined a forward-looking manufacturer, a myopic retailer, low-carbon goodwill, and product-specific low-carbon awareness under cap-and-trade regulation; control parameterization and constrained retailer responses yield selected numerical candidates with Softplus smoothing. Carbon-price transmission depended on the emission-effort regime: Effort remained at its upper bound in the tested low-cost setting, whereas mean effort declined modestly with carbon price in the higher-cost interior regimes. Across these regimes, higher carbon prices raise mean wholesale and retail prices, reduce mean demand, and increase the retailer's mean disadvantageous profit gap. Stronger inequity aversion under high profit-comparison pressure induces preemptive wholesale-price concessions. An exact positive-part benchmark preserves this direction while revealing smoothing sensitivity in near-kink activation and response magnitudes. A composite contract combined marginal-cost wholesale pricing, promotion sharing, direct emission-incentive support, and fixed redistribution. Under the tested discretization and contract conditions, independently selected contract paths approached the discrete integrated reference and satisfied material-profit and post-fee behavioral-utility participation. These findings revealed a price-coordination/emission-incentive conflict and supported numerical contract implementation within the specified model and finite checks; they do not establish general continuous-time coordination.

Keywords: low-carbon supply chain; cap-and-trade mechanism; disadvantageous inequity aversion; dynamic Stackelberg game; composite coordination contract; control parameterization method
Mathematics Subject Classification: 91A65, 91B76, 49N90, 90B50

1. Introduction

Benjaafar et al. [1] incorporated carbon emissions into classical operational models; Hua et al. [2] examined inventory management under carbon trading; Du et al. [3] studied an emission-dependent supply chain under cap-and-trade regulation; and Xu et al. [4] reviewed supply chain management under cap-and-trade mechanisms. In a manufacturer-led channel, the central issue is therefore not only whether carbon regulation changes upstream incentives, but also whether those incentives can be transmitted without worsening the downstream member's perceived share of channel returns. A policy or low-carbon decision may improve the manufacturer's carbon-related payoff while enlarging the retailer's disadvantageous relative-profit gap. Moreover, if the retailer is sensitive to disadvantageous inequity, that distributional change affects pricing and promotion, which the manufacturer anticipates when setting wholesale and emission-reduction paths. This creates a dynamic incentive–allocation conflict: Decisions that strengthen upstream low-carbon incentives can induce downstream behavioral responses that reshape prices, promotion, demand, and the leader's own path choice. A material-profit model alone omits this feedback through vertical profit comparison.

The tension is intertemporal because emission reduction and promotion affect accumulated market states as well as current demand. Dynamic goodwill studies explain this persistence [5–7]. The Fairness-channel theory establishes that relative-profit preferences change retail pricing and anticipated wholesale terms: Cui et al. [8] provided the analytical antecedent to the effective-price transformation used below. The analysis embeds that established pricing logic in a dynamic low-carbon setting to examine how policy-induced profit allocation and accumulated market states affect operating responses and coordination incentives.

The manufacturer commits to wholesale-price and emission-reduction paths, while the retailer chooses price and promotion pointwise to maximize current utility. Low-carbon goodwill and product-specific low-carbon awareness carry past effort into future demand. The awareness state captures recognition of observable low-carbon product attributes, rather than broad societal environmental awareness. In Section 4, we describe the constrained response and control-parameterization scheme.

Accordingly, two questions guide the analysis. First, how does cap-and-trade-induced redistribution of channel profit affect the retailer's weighted relative-profit gap and the resulting dynamic pricing and promotion response? Second, can channel price coordination reduce double marginalization without eroding the manufacturer's emission incentive, and how does the tested contract address that trade-off? The established fairness-adjusted pricing representation helps interpret the wholesale concessions connecting these questions.

The analysis examines two model-specific mechanisms without claiming novelty from the coexistence of carbon regulation, dynamic states, and inequity aversion. First, carbon policy reallocates vertical profit and changes the retailer's disadvantageous relative-profit signal. The resulting pricing and promotion response feeds into the manufacturer's anticipated wholesale-price and emission-reduction choices. This policy–behavior channel depends on disadvantageous inequity aversion and open-loop manufacturer leadership. In the tested $\eta_m \times p_c$ grid, low-cost effort is saturated at $E_{\max}$, whereas the two higher-cost regimes are interior. The common price-allocation pattern therefore extends beyond the original boundary case, while the effort response remains regime dependent (Section 5.3.1).

Second, effective marginal-cost wholesale pricing mitigates double marginalization but removes the manufacturer's demand-side wholesale margin. The C3 validation tests fixed promotion sharing, direct emission-incentive support, and redistribution against a discrete integrated reference. In Section 6.7, we compare complete paths and check accounting, material-profit participation, and post-fee behavioral-utility participation under frozen clauses, with pointwise responses and effective effort deviations assessed separately. These checks support the implemented bundle without establishing the universal necessity of its components.

Proposition 2 adapts the disadvantaged-fairness pricing logic of Cui et al. [8] to carbon-adjusted marginal cost, promotion, and the original feasibility constraints. This supporting analytical bridge represents the retailer's exact positive-part objective only on the activated branch; it is neither a new fairness-pricing result nor a finite-k or intertemporal leader-equilibrium formula. State accumulation and manufacturer anticipation belong to the surrounding model.

The remainder of the paper is organized as follows: In Section 2, we review the related literature. In Section 3, we formulate the continuous-time Stackelberg model. In Section 4, we present the numerical solution framework. In Section 5, we report the numerical simulations and mechanism analyses. In Section 6, we report new fixed-contract validation, including paired-path proximity, same-path material and utility participation, and finite effort checks. In Section 7, we conclude the paper and discuss managerial implications and future research directions.

2. Literature review

Three streams provide the basis for the analysis: carbon regulation and operating incentives, intertemporal market-state accumulation, and relative-payoff preferences in channel decisions. We use these streams to formulate the policy–behavior question and the associated coordination conflict.

2.1. Low-carbon supply chain decisions under carbon regulation

Carbon regulation has become a core issue in low-carbon supply chain management. Benjaafar et al. [1] incorporated carbon emissions into classical operational models; Hua et al. [2] examined inventory management under carbon trading; Du et al. [3] studied an emission-dependent supply chain under cap-and-trade regulation; and Xu et al. [4] reviewed supply chain management under cap-and-trade mechanisms. These studies show that carbon policies reshape operational decisions through emission costs, carbon-trading payoffs, price transmission, and quota allocation.

Another related stream studies low-carbon investment and coordination. Zhou and Ye [9] analyzed joint emission-reduction strategies and contract design in a dual-channel supply chain, while Wang and Zhao [10] showed that emission reduction and low-carbon promotion can be improved through cost-sharing mechanisms. Peng et al. [11] studied low-carbon supply chain decisions under cap-and-trade and subsidy policy; Ren and Hu [12] examined coordination with a wholesale-price constraint under government subsidies; Yan and Ni [13] analyzed pricing and low-carbon decisions under uncertainty and cap-and-trade regulation; and Lin et al. [14] compared operational strategies under two carbon-trading pathways. These papers provide the policy and operational foundation. For this analysis, we ask how the resulting vertical allocation of profit enters a retailer's inequity-sensitive response over time.

Zhu et al. [15] compared grandfathering and benchmarking in a manufacturer–retailer supply chain where green technology, recycling, and promotion jointly build green goodwill. Their infinite-horizon

differential game used fixed unit marginal profits and excluded pricing decisions; the analysis solved Hamilton–Jacobi–Bellman equations and extended them to stochastic goodwill. Moreover, equal retailer promotion across the no-cap-and-trade and two allocation regimes does not imply policy-independent retailer profits, which are affected indirectly through goodwill. The model endogenizes wholesale and retail prices alongside promotion, linking carbon-policy-induced profit allocation to the retailer's disadvantageous relative-profit signal.

2.2. Dynamic low-carbon state accumulation

Low-carbon demand depends on current decisions and accumulated market states. The Nerlove–Arrow goodwill model [5] provides the classical foundation for modeling how current effort affects future demand through state accumulation. In low-carbon supply chains, Xu et al. [6] introduced low-carbon goodwill into a continuous-time differential game, Wang and Zhu [7] examined long-term emission-reduction decisions under different carbon permit allocation rules, and Wang et al. [16] studied dynamic pricing, green effort, and coordination in a three-echelon green supply chain.

Consumer-side low-carbon perception has also been modeled dynamically. Zhang and Yu [17] studied cooperative emission reduction with reference low-carbon effects and low-carbon goodwill, Wu et al. [18] examined reference effects under different quota allocation methods, and Gao et al. [19] considered customer-preference updating in low-carbon supply chain incentive design. Our model uses $R(t)$ for product-specific low-carbon awareness accumulated from observable emission-reduction information. It enters demand additively rather than serving as a gap-based reference utility term; its restricted information mechanism is explained in Section 3.3.1.

Zhu et al. [20] studied endogenous wholesale and retail pricing in an infinite-horizon feedback differential game with a manufacturer and two competing retailers. Green technology, recycling, and marketing build green brand image under carbon tax and cap-and-trade policies. Their comparison separates retailer alliance formation from shifts in channel power: Under their assumptions, an alliance leaves the wholesale price unchanged while the manufacturer remains the leader, whereas Nash play or alliance leadership yields a lower wholesale price. The model keeps manufacturer leadership fixed and examines anticipated responses to the retailer's disadvantageous inequity aversion.

2.3. Behavioral preferences and supply chain coordination

Behavioral operations research shows that supply chain members may care about relative payoff, fairness, reciprocity, risk, or loss aversion rather than only absolute profit. Fehr and Schmidt [21] and Bolton and Ockenfels [22] provided the classical foundations for inequity aversion and equity-based preferences. In supply chain settings, Cui et al. [8] derived the retailer's branch-dependent pricing response and the manufacturer's anticipated wholesale decision. Normalizing their disadvantageous-fairness branch yields the core effective-wholesale-price adjustment underlying Eq (22); their analysis also relates fairness concerns to lower wholesale terms. This is a substantive analytical antecedent to Proposition 2. Caliskan-Demirag et al. [23] examined channel coordination with fairness concerns and nonlinear demand, while Ho et al. [24] studied distributional and peer-induced fairness in contract design. Loch and Wu [25] experimentally studied social preferences and supply chain performance, while Chen et al. [26] examined supply chain fairness. Related analytical studies examine loss aversion, power imbalance, supply uncertainty, and marketing effort in supply chain contracting [27–29]. Katok and Pavlov [30] reported a

laboratory study of fairness in supply chain contracts; Qin et al. [31] analyzed fairness concerns under private cost information; and Pavlov et al. [32] studied optimal contracting with asymmetric information about fairness.

Low-carbon behavioral studies address several closely related decisions. Zhou et al. [33] studied advertising and emission-reduction cost sharing under fairness concerns. Qian et al. [34] examined channel coordination between a socially responsible manufacturer and a fair-minded retailer under cap-and-trade regulation. Xia et al. [35] considered reciprocal preferences and consumers' low-carbon awareness in a cap-and-trade supply chain. Zhang and Yi [36] examined loss-averse competitive manufacturers with reference dependence under cap-and-trade policy. These positive descriptions follow the papers' stated research settings; they do not establish the absence of any particular pricing or coordination mechanism.

Dynamic and contractual antecedents are also directly relevant. Zhang and Yu [37] modeled reference low-carbon level and goodwill as dynamic states, with manufacturer emission reduction, retailer promotion, fairness concerns, and cost-/revenue-sharing coordination. Their reference state enters demand through the difference between current emission reduction and the reference level. Xia et al. [38] studied emission reduction and promotion in a differential game with consumer low-carbon awareness and social preferences, including relationship and status preferences. Yu et al. [39] analyzed a three-echelon cap-and-trade channel with manufacturers' fairness concerns, low-carbon efforts, and emission-reduction cost sharing. Shi et al. [40] analyzed reciprocal behavior and advertising/emission-reduction cost-sharing contracts under cap-and-trade, including conditions under which advertising cooperation alone can coordinate their model. Wu et al. [41] examined green investment, marketing efforts, and retailer risk aversion under carbon tax policy, while Chen et al. [42] studied low-carbon coordination with Nash bargaining fairness. These antecedents preclude treating the coexistence of behavioral preferences, low-carbon decisions, dynamics, or coordination contracts as the contribution.

2.4. Literature synthesis and research positioning

The alliance and allocation-rule studies of Zhu et al. [15, 20] therefore provide distinct benchmarks: channel power with endogenous prices, and carbon-policy incentives with fixed unit marginal profits. Building on these and the behavioral antecedents above, we examine two model-specific mechanisms: Policy-induced profit reallocation feeds through the retailer's disadvantageous relative-profit signal into pricing, promotion, and anticipated manufacturer decisions; eliminating the manufacturer's wholesale demand margin mitigates double marginalization while weakening demand-side emission incentives. Established fairness-adjusted pricing provides an analytical bridge between carbon-adjusted costs and these dynamic responses. Moreover, we do not treat the coexistence of model features, the open-loop formulation, the two accumulated states, or the bundling of contract clauses as independent novelties. The contract is evaluated for the price-coordination/emission-incentive conflict within the stated model and numerical evidence without asserting literature-wide priority.

Table 1 provides descriptive background on selected model features. Its categories do not establish novelty or an exhaustive classification of the literature. In particular, the construct-specific state column distinguishes additive product-specific low-carbon awareness from a reference-low-carbon state; it does not count dynamic states.

Proposition 2 links profit comparison to wholesale concessions using established pricing logic, while the exact-hinge benchmark tests the direction without Softplus regularization. In Sections 4.4

and 6.7, we distinguish the analytical results from the numerical evidence on policy transmission and fixed-contract implementation; the latter does not establish that every contract component is necessary. Comparisons with closely related studies available only through authoritative abstracts remain limited to positively stated features, and unavailable full text is not evidence of absence.

Table 1. Descriptive comparison of selected model features.

Literature	Carbon policy	Dynamics	Behavior	Goodwill + additive awareness	Contract
Benjaafar et al. [1]	√	–	–	–	–
Wang and Zhao [10]	–	√	–	–	√
Xu et al. [6]	–	√	–	–	√
Wang and Zhu [7]	√	√	–	–	–
Shi et al. [40]	√	–	√	–	√
Wu et al. [18]	√	√	–	–	–
Zhang and Yu [37]	–	√	√	–	√
Zhou et al. [33]	–	–	√	–	√
Yu et al. [39]	√	–	√	–	√
Chen et al. [42]	–	–	√	–	√
Zhu et al. [20]	√	√	–	–	–
Zhu et al. [15]	√	√	–	–	–
This paper	√	√	√	√	√

*Note: √ indicates reported inclusion of a feature. A dash leaves the feature unclassified under the stated heading and is not evidence of its absence. The state column refers specifically to low-carbon goodwill together with additive product-specific low-carbon awareness, not merely two dynamic states. Zhang and Yu [37] explicitly model both goodwill and a reference-low-carbon state; their demand depends on the gap between current emission reduction and that reference level. The present awareness state instead contributes positively and additively to demand. This distinction is descriptive and does not establish novelty.

3. Model formulation

3.1. Model overview and Stackelberg structure

In this paper, we formulate an open-loop Stackelberg model for a two-echelon low-carbon supply chain consisting of one manufacturer and one retailer. The manufacturer is the channel leader and chooses the wholesale-price path $W(t)$ and emission-reduction effort path $E(t)$ over the planning horizon. The retailer is the follower and, given the manufacturer's current decisions and the current state variables, chooses the retail price $P(t)$ and low-carbon promotional effort $A(t)$ pointwise.

The model consists of two nested decision problems. At the lower level, the retailer solves

$$(P^*(t), A^*(t)) \in \arg\max_{P(t),A(t)} \{U_r^s(t) : Q(t) \geq 0,\ P(t) \geq W(t),\ A_{\min} \leq A(t) \leq A_{\max}\}.$$

At the upper level, anticipating the retailer's response, the manufacturer solves

$$\begin{aligned} \max_{W(t),E(t)} \quad & J_m = \int_0^T e^{-\rho t}\pi_m(t)\,dt \\ \text{s.t.} \quad & \dot{G}(t) = \rho_{GE}E(t) + \rho_{GA}A^*(t) - \delta_G G(t), \\ & \dot{R}(t) = \rho_{RE}E(t) - \delta_R R(t), \\ & E_{\min} \leq E(t) \leq E_{\max}, \\ & (P^*(t), A^*(t)) \text{ solves the retailer's lower-level response problem.} \end{aligned}$$

The demand function, state dynamics, profit functions, inequity-averse utility, and feasibility constraints are specified below as primitives of this Stackelberg model. This structure captures the

dynamic interaction among emission reduction, promotion, wholesale–retail pricing, carbon trading, state accumulation, and channel profit comparison, and it provides the basis for the composite coordination contract developed in Section 6.

3.2. Model assumptions

To focus on the dynamic emission-reduction and behavioral response mechanisms, the model is built on the following assumptions.

Assumption 1. Continuous-time open-loop leader–follower structure. The manufacturer commits at the beginning of the horizon to time-indexed $W(t)$ and $E(t)$, interpreted as channel-policy and emission-investment decisions with intertemporal consequences. The retailer chooses $P(t)$ and $A(t)$ as shorter-horizon operating decisions and maximizes current utility. This deliberate asymmetry represents an organizational division in which wholesale policy and emission investment are long-horizon upstream choices, while retail pricing and promotion are managed as current-margin operating decisions. It is intended as a stylized representation of manufacturer-led channels in which wholesale terms and decarbonization roadmaps are set on a seasonal or contractual horizon, while store-level pricing and promotion can be adjusted more frequently. Although $A(t)$ enters the goodwill dynamics, the retailer does not attach a continuation value to that state effect; the manufacturer anticipates the induced retailer response and its consequences for state evolution. Thus, retailer myopia is an economic scope choice rather than a computational requirement. Both members know the market, cost, demand, and behavioral parameters, and $G(t), R(t)$ are observable; this information does not give the retailer an intertemporal objective. In Section 3.5, we discuss commitment and the equilibrium implications of this horizon asymmetry.

Assumption 2. Demand is affected by price, effort, goodwill, and awareness. Market demand depends on the retail price, promotional effort, emission-reduction effort, low-carbon goodwill, and product-specific low-carbon awareness:

$$Q(t) = q_0 - b_p P(t) + b_A A(t) + b_E E(t) + b_G G(t) + b_R R(t). \tag{1}$$

Here, $q_0 > 0$ is the potential market size, $b_p > 0$ is the price sensitivity coefficient, and $b_A, b_E, b_G, b_R > 0$ measure the demand effects of promotion, emission reduction, low-carbon goodwill, and product-specific low-carbon awareness, respectively. Economic feasibility requires

$$Q(t) \geq 0.$$

The state $R(t)$ denotes product-specific low-carbon awareness: accumulated recognition of the focal product's low-carbon attributes associated with observable emission-reduction information. It is not broad societal environmental awareness or a reference benchmark in a gap-based utility; it enters demand additively. Education, social norms, public campaigns, and other time-varying exogenous awareness shocks lie outside its endogenous baseline mechanism. The initial condition R_0 can capture inherited product-level awareness at the start of the planning horizon, but subsequent exogenous awareness inflows are not represented in the baseline dynamics. Thus, the specification does not assume that broad environmental awareness is generated solely by the manufacturer's emission-reduction effort. Hereafter, awareness refers only to this product-specific state.

Assumption 3. Low-carbon goodwill and product-specific low-carbon awareness evolve dynamically. Low-carbon goodwill $G(t)$ captures accumulated market-level image from emission

reduction and promotion. The awareness state $R(t)$ captures accumulated recognition of observable, credible information about emission-reduction performance. Both states decay. Conditional on the inherited stock R_0, the baseline makes subsequent changes in $R(t)$ endogenous only to the emission-reduction information channel. Promotion's accumulated influence is assigned to goodwill rather than awareness. This separation is a modeling restriction used to keep the two state channels identifiable; it is not a claim that promotion, social diffusion, or policy communication cannot affect awareness in practice. In Section 3.3.1, we state the dynamics and their limitations.

Assumption 4. The retailer has disadvantageous inequity aversion based on channel profit comparison. The manufacturer maximizes intertemporal material profit. The behavioral focus is the downstream follower's perceived disadvantage relative to the manufacturer's weighted profit reference. This one-sided specification is most relevant as a stylized manufacturer-led channel in which the downstream member observes or forms beliefs about upstream returns and reacts when its own payoff falls below a weighted upstream reference. It isolates the response to perceived upstream advantage and the leader's anticipation of that response; it does not assert that manufacturers lack fairness preferences. The baseline therefore penalizes disadvantageous comparison only. Manufacturer fairness, bilateral fairness, and advantageous inequity aversion would introduce additional preference branches and answer different bargaining questions, so they are excluded rather than implicitly assumed irrelevant. Their possible effects are discussed in Section 3.4.1.

Assumption 5. Control variables satisfy economic feasibility constraints. The control variables satisfy

$$E_{\min} \le E(t) \le E_{\max}, \qquad A_{\min} \le A(t) \le A_{\max}, \qquad P(t) \ge W(t). \tag{2}$$

The constraint $P(t) \ge W(t)$ rules out inverted pricing. Together with the nonnegative-demand constraint, it forms the endogenous economic boundary of the retailer's pointwise response problem. From Eq (1), nonnegative demand also implies the endogenous price upper bound

$$P(t) \le \frac{q_0 + b_A A(t) + b_E E(t) + b_G G(t) + b_R R(t)}{b_p}.$$

Thus, the feasible retail price is bounded by market demand tolerance rather than by an arbitrary economic price cap. If the emission-reduction effort reaches $E_{\min}$ or $E_{\max}$, the corresponding optimality condition should be interpreted through boundary KKT conditions rather than interior first-order equalities.

3.3. State dynamics and profit functions

3.3.1. Dynamic evolution of state variables

Low-carbon goodwill evolves according to

$$\dot{G}(t) = \rho_{GE} E(t) + \rho_{GA} A(t) - \delta_G G(t), \tag{3}$$

where ρ_{GE} and ρ_{GA} measure the effects of emission-reduction effort and promotional effort on goodwill, respectively, and δ_G is the goodwill decay rate.

Product-specific low-carbon awareness evolves according to

$$\dot{R}(t) = \rho_{RE} E(t) - \delta_R R(t), \tag{4}$$

where ρ_{RE} measures the effect of emission-reduction effort on awareness, and δ_R is the awareness decay rate. The initial states are

$$G(0) = G_0, \qquad R(0) = R_0.$$

Beyer et al. [43] provided field-experimental evidence that product-level carbon-footprint information can affect consumer food choices. This supports considering a product-information channel, but does not validate the particular accumulation equation or the separation of promotion and awareness used here. Equation (4) therefore represents only the endogenous accumulation of product-specific low-carbon awareness generated by observable emission-reduction performance. The link from E to recognition assumes that such information is credible and available; verification is not modeled. Promotion A primarily builds goodwill in Eq (3). Assigning its accumulated baseline effect to G avoids attributing the same assumed promotional channel to both states. Time-varying public campaigns, social diffusion, intrinsic preference shifts, and promotion-to-awareness spillovers are deliberately excluded from the baseline rather than treated as zero in reality. A broader specification could use $\dot{R} = \rho_{RE}E + \rho_{RA}A + \xi_R(t) - \delta_R R$, where $\xi_R(t)$ captures exogenous awareness inflow. Neither $\rho_{RA}A(t)$ nor $\xi_R(t)$ is included or evaluated in the reported computations, so the numerical results should not be interpreted as evidence about the evolution of broad societal environmental awareness.

3.3.2. Manufacturer's instantaneous profit function

The manufacturer's instantaneous profit consists of wholesale revenue, production cost, emission-reduction investment cost, and carbon-trading payoff. Let c_m denote unit production cost, η_m the emission-reduction cost coefficient, e_{unit} the baseline unit emission coefficient, ϕ_E the emission-offset coefficient of emission-reduction effort, C_{cap} the carbon quota, and p_c the carbon trading price. The manufacturer's net emissions are

$$M(t) = e_{\text{unit}}Q(t) - \phi_E E(t).$$

The manufacturer's instantaneous profit is

$$\pi_m(t) = [W(t) - c_m - p_c e_{\text{unit}}]\, Q(t) - \frac{1}{2}\eta_m E^2(t) + p_c C_{\text{cap}} + p_c \phi_E E(t). \tag{5}$$

Equation (5) shows that $p_c e_{\text{unit}}$ is the per-unit carbon opportunity cost of sales, so the effective unit marginal cost is $c_m + p_c e_{\text{unit}}$. It also shows that emission-reduction effort generates a marginal carbon-trading payoff $p_c \phi_E$.

3.3.3. Retailer's instantaneous material profit function

The retailer's material profit is its monetary profit before the inequity-aversion adjustment. It comes from the terminal sales margin after deducting promotional cost:

$$\pi_r(t) = [P(t) - W(t)]\, Q(t) - \frac{1}{2}\eta_r A^2(t), \tag{6}$$

where η_r is the promotional cost coefficient. This material profit forms the basis for the retailer's channel profit-comparison-based inequity-averse utility and for the promotion cost-sharing contract developed later.

3.4. Retailer's utility function and lower-level response problem

3.4.1. Channel profit-comparison-based inequity-averse utility

Motivated by inequity-aversion and fairness-concern models, we assume that the retailer cares about its own material profit and its relative profit position compared with the manufacturer. Since the model focuses on vertical channel profit comparison in a manufacturer-led structure, the manufacturer's profit adjusted by a subjective comparison weight is used as the retailer's profit reference level, namely $\omega_\pi \pi_m(t)$.

The perceived disadvantageous inequity gap is defined as

$$\Delta\Pi(t) = \omega_\pi \pi_m(t) - \pi_r(t). \tag{7}$$

Here, ω_π denotes the retailer's subjective weight assigned to the manufacturer's profit in channel profit comparison. When $\omega_\pi = 1$, the retailer compares its profit directly with the manufacturer's material profit. When $\omega_\pi > 1$, the retailer perceives a stronger upstream profit advantage for the same manufacturer profit. Thus, a positive perceived inequity gap does not require the retailer's actual material profit to be lower than the manufacturer's actual material profit; it is sufficient that the retailer's profit is below the weighted manufacturer-profit reference level.

This specification retains the disadvantageous component of a Fehr–Schmidt-type inequity preference [21]. When $\Delta\Pi(t) > 0$, the retailer perceives itself to be in a disadvantageous relative profit position and incurs an inequity penalty. When $\Delta\Pi(t) \leq 0$, the exact positive-part term is inactive; no advantageous-inequity penalty is modeled. This restriction isolates a follower's response to perceived upstream advantage. Allowing fairness preferences on the manufacturer side, as considered in the related literature [39], on both sides, or in the advantageous direction could change responses and contract incentives. Those alternatives are outside this model; their outcomes are not inferred from the one-sided specification.

Let $\lambda_L \geq 1$ denote the retailer's disadvantageous inequity-aversion coefficient. The retailer's instantaneous inequity-averse utility is

$$U_r(t) = \pi_r(t) - (\lambda_L - 1)\max\{\Delta\Pi(t), 0\}. \tag{8}$$

When $\lambda_L = 1$, the retailer reduces to a material-profit maximizer. When $\lambda_L > 1$, the retailer incurs an additional utility penalty from the perceived disadvantageous relative profit gap. A larger λ_L represents stronger sensitivity to disadvantageous inequity in channel profit comparison.

3.4.2. Softplus approximation of the inequity-aversion term

The positive-part function in Eq (8) is non-differentiable at $\Delta\Pi(t) = 0$. To obtain a differentiable objective for the numerical solution, we use a Softplus approximation. The relative profit gap is first nondimensionalized as

$$\widehat{\Delta\Pi}(t) = \frac{\Delta\Pi(t)}{S_\pi},$$

where $S_\pi > 0$ is the monetary scale of the smoothing approximation. The analytical profit identities are stated in the original monetary units. For numerical evaluation, monetary profit flows and contract transfers are divided by $S_{\text{rep}} = 100$ before constructing the behavioral utility; numerical π_m, π_r, and $\Delta\Pi$ denote these normalized quantities. Prices, efforts, states, and demand are not divided by this scale.

Given the grid $t_0, t_1, \dots, t_N$, S_π is calibrated in the same normalized monetary units from the no-penalty benchmark ($\lambda_L = 1$):

$$S_\pi = \frac{1}{2(N+1)} \sum_{i=0}^{N} \left(|\pi_m(t_i)| + |\pi_r(t_i)| \right).$$

This scale is evaluated once on the benchmark path and then held fixed at $S_\pi = 8.335937$ in the numerical comparisons and contract validation. The reporting and behavioral calculations use the same normalized monetary flows; S_π is not a second division of prices or physical quantities. Analytical transfer and marginal-incentive formulas must likewise be evaluated in a common monetary unit.

The Softplus function is defined as

$$\mathrm{sp}_k(x) = \frac{1}{k} \ln(1 + \exp(kx)), \qquad k > 0. \tag{9}$$

The smoothed retailer utility is

$$U_r^s(t) = \pi_r(t) - (\lambda_L - 1) S_\pi \, \mathrm{sp}_k\left(\widehat{\Delta\Pi}(t)\right). \tag{10}$$

For every real x, the approximation error satisfies

$$\mathrm{sp}_k(x) - [x]_+ = \frac{\ln(1 + e^{-k|x|})}{k}, \qquad 0 \le \mathrm{sp}_k(x) - [x]_+ \le \frac{\ln 2}{k}.$$

Consequently, at a fixed state and decision point, for $\lambda_L \ge 1$,

$$0 \le U_r(t) - U_r^s(t) \le \frac{(\lambda_L - 1) S_\pi \ln 2}{k}.$$

This is a pointwise utility-approximation bound in the chosen monetary units; it does not bound the difference between equilibrium paths. Increasing k reduces the pointwise approximation bias and increases curvature near the kink. For finite k, the Softplus penalty remains positive even at a negative gap when $\lambda_L > 1$. The baseline numerical specification uses $k = 8$. Therefore, in Section 5.4, we combine finite-k sensitivity with an exact positive-part benchmark so that near-kink approximation effects can be assessed without treating the pointwise bound as an equilibrium-path bound or assuming convergence of the leader equilibrium as k increases.

3.4.3. Retailer's lower-level response problem and uniqueness

Given the current states $G(t)$ and $R(t)$, and the manufacturer's current decisions $W(t)$ and $E(t)$, the retailer chooses $P(t)$ and $A(t)$ to maximize the smoothed instantaneous utility:

$$\begin{aligned} \max_{P(t), A(t)} \quad & U_r^s(t) \\ \text{s.t.} \quad & Q(t) \ge 0, \quad P(t) \ge W(t), \\ & A_{\min} \le A(t) \le A_{\max}. \end{aligned} \tag{11}$$

The nonnegative-demand constraint implies the endogenous price upper bound

$$P(t) \le \frac{q_0 + b_A A(t) + b_E E(t) + b_G G(t) + b_R R(t)}{b_p}.$$

Thus, the retailer's feasible price is bounded by market demand tolerance rather than by an arbitrary economic price cap.

Proposition 1 (Existence and uniqueness of the retailer's pointwise response)**.** *For given $G(t)$, $R(t)$, $W(t)$, and $E(t)$, suppose that the feasible set in Eq* (11) *is nonempty and that*

$$2b_p\eta_r > b_A^2.$$

Then the retailer's smoothed pointwise response problem admits a unique optimal solution.

Proof. For fixed $G(t)$, $R(t)$, $W(t)$, and $E(t)$, the demand function is affine in $P(t)$ and $A(t)$. The retailer's material profit has the Hessian matrix

$$H_{\pi_r} = \begin{pmatrix} -2b_p & b_A \\ b_A & -\eta_r \end{pmatrix}.$$

Under $2b_p\eta_r > b_A^2$, H_{π_r} is negative definite. Hence, $\pi_r(t)$ is strictly concave in $(P(t), A(t))$.

For fixed manufacturer decisions and states, the manufacturer's profit is affine in $(P(t), A(t))$. Therefore, $\Delta\Pi(t) = \omega_\pi \pi_m(t) - \pi_r(t)$ is convex in $(P(t), A(t))$. Since the Softplus function is convex and nondecreasing, its composition with $\widehat{\Delta\Pi}(t)$ is convex. The smoothed inequity-aversion penalty is therefore convex, and subtracting it from the strictly concave material profit preserves strict concavity of $U_r^s(t)$.

The feasible set in Eq (11) is defined by linear constraints and a bounded promotional-effort interval. It is convex and compact whenever it is nonempty. A strictly concave continuous objective over a nonempty compact convex feasible set admits a unique maximizer. This completes the proof.

Proposition 1 establishes uniqueness only for the retailer's pointwise inner response under fixed manufacturer decisions and current states. The manufacturer's intertemporal problem remains non-convex after control parameterization and is therefore examined through selected feasible numerical candidates, with retailer-response and outer termination diagnostics distinguished in Section 4.

3.5. The complete open-loop Stackelberg model

As the supply-chain leader, the manufacturer chooses $W(t)$ and $E(t)$ over the planning horizon to maximize discounted intertemporal profit:

$$J_m = \int_0^T e^{-\rho t} \pi_m(t)\, dt, \tag{12}$$

where ρ is the discount rate and T is the planning horizon. The retail price and promotional effort entering $\pi_m(t)$ are determined by the retailer's pointwise optimal response.

The manufacturer's intertemporal problem is

$$\begin{aligned} \max_{W(t),E(t)} \quad & J_m \\ \text{s.t.} \quad & \dot{G}(t) = \rho_{GE}E(t) + \rho_{GA}A^*(t) - \delta_G G(t), \\ & \dot{R}(t) = \rho_{RE}E(t) - \delta_R R(t), \\ & G(0) = G_0, \quad R(0) = R_0, \\ & E_{\min} \le E(t) \le E_{\max}, \\ & (P^*(t), A^*(t)) \text{ solves Eq (11).} \end{aligned} \tag{13}$$

Equivalently, for each t,

$$(P^*(t), A^*(t)) \in \arg\max_{P(t),A(t)} \{U_r^S(t) : (P(t), A(t)) \text{ satisfies Eq (11)}\}.$$

By Proposition 1, when the retailer's feasible set is nonempty and the concavity condition holds, $(P^*(t), A^*(t))$ is uniquely determined for given $G(t)$, $R(t)$, $W(t)$, and $E(t)$. The manufacturer's decisions affect current profit and future demand through the evolution of low-carbon goodwill and product-specific low-carbon awareness, while the retailer responds myopically at each time point according to the current state, current manufacturer decisions, and the channel profit-comparison mechanism.

Because promotion enters $\dot{G}(t)$, the horizon assumption affects the lower-level optimality conditions rather than merely their interpretation. In this pointwise response, the marginal condition for $A(t)$ contains only contemporaneous utility effects and no retailer-side continuation-value term associated with future goodwill. A forward-looking retailer would instead internalize the effect of current promotion on future G, demand, and downstream profit through a state shadow value. The manufacturer nevertheless internalizes the state dynamics in its own intertemporal objective and anticipates the retailer's pointwise response when choosing $W(t)$ and $E(t)$. Dynamic internalization is therefore asymmetric, not absent. A forward-looking downstream objective could alter $A(t)$, $P(t)$, and, through the leader's anticipation, the resulting $W(t)$ and $E(t)$ paths; its direction cannot be signed without solving the alternative dynamic game.

The solution concept is an open-loop leader–follower path with pointwise myopic retailer responses. Open-loop commitment is chosen because the research question concerns ex ante wholesale-price and decarbonization path commitments and their interaction with accumulated market states, rather than adaptive state-contingent contracting after every state realization. Precommitted time paths provide a benchmark for long-horizon wholesale-price arrangements and emission-reduction roadmaps when commitments are credible and structural parameters are relatively stable. The manufacturer does not choose state-feedback rules $W(G, R, t)$ or $E(G, R, t)$, even though the retailer observes the current states when responding. Feedback or receding-horizon decisions could adapt to realized G, R and produce different paths; no such game is solved here. The computed paths are selected feasible numerical candidates under the specified control parameterization, Softplus smoothing, time grid, multi-start procedure, and tolerances. Feasibility, retailer-response diagnostics, and repeatability of the reported candidate paths do not certify manufacturer outer stationarity. Non-convexity permits other candidates; neither global optimality nor insensitivity to the solution concept is established. At $E_{\min}$ or $E_{\max}$, analytical optimality conditions take the boundary KKT form, but a boundary hit alone is not a verified leader boundary certificate.

4. Control-parameterization-based numerical solution framework

The manufacturer's intertemporal optimization contains a constrained, pointwise retailer response and state equations linking current choices to future demand. The nonsmooth inequity-aversion term adds numerical difficulty. Control parameterization reduces this open-loop problem to a finite-dimensional nonlinear program. In Section 4.4, we define the evidence supplied by its selected feasible paths.

4.1. Control parameterization and nested response

Given $G(t)$, $R(t)$, $W(t)$, and $E(t)$, the retailer solves the constrained pointwise response problem in Eq (11). The manufacturer's control paths are approximated by exponential-adjustment functions:

$$W(t;\theta_W) = \theta_{W,1} + \theta_{W,2}e^{-\theta_{W,3}t}, \qquad \widehat{E}(t;\theta_E) = \theta_{E,1} + \theta_{E,2}e^{-\theta_{E,3}t}. \tag{14}$$

The full parameter vector is $\theta = (\theta_W, \theta_E) \in \mathbb{R}^6$, and emission-reduction effort is projected onto its feasible interval:

$$E(t;\theta_E) = \mathrm{proj}_{[E_{\min},E_{\max}]}\big(\widehat{E}(t;\theta_E)\big). \tag{15}$$

Boundary segments are interpreted through KKT complementarity rather than interior first-order equalities. After parameterization, the outer problem searches over θ; for any candidate θ, the manufacturer controls are generated on the grid, the retailer's pointwise response is solved, and the state variables are advanced forward.

4.2. Time discretization and state integration

The horizon $[0, T]$ is divided into N equal intervals:

$$t_i = i\Delta t, \quad i = 0, 1, \dots, N, \qquad \Delta t = \frac{T}{N}. \tag{16}$$

At node t_i, the controls W_i and E_i are generated and the retailer obtains (P_i^*, A_i^*). Let $x = (G, R)^\top$. The state equation used for numerical integration is

$$f(x,t;\theta) = \begin{pmatrix} \rho_{GE}E(t;\theta_E) + \rho_{GA}A^*(x,t;\theta) - \delta_G G \\ \rho_{RE}E(t;\theta_E) - \delta_R R \end{pmatrix}. \tag{17}$$

In Chapter 5, fourth-order Runge–Kutta (RK4) integration recomputes controls and retailer responses at intermediate stages. New I and C3 instead hold nodal A_i, E_i fixed within each state step (Section 6.7.1). Discounted payoffs are approximated by the composite trapezoidal rule, consistent with `trapz`:

$$J_m^h(\theta) = \mathrm{trapz}\left(\{t_i\}_{i=0}^N, \{e^{-\rho t_i}\pi_{m,i}\}_{i=0}^N\right). \tag{18}$$

The same quadrature rule is used for the retailer's material payoff and the channel-level payoff.

4.3. Feasibility diagnostics and outer objective

At node t_i, the main feasibility residual is

$$r_i = \max\left\{\max(0, -Q_i),\ \max(0, W_i - P_i^*),\ \max(0, A_{\min} - A_i^*, A_i^* - A_{\max})\right\}. \tag{19}$$

The theoretical target is the constrained utility maximization in Eq (11). In the residual-based Chapter 5 baseline, finite-k sensitivity, and cost-regime experiments, bounded `lsqnonlin` minimizes the augmented stationarity residual

$$\left(\frac{\partial U_r^s}{\partial P},\ \frac{\partial U_r^s}{\partial A},\ 10\,\mathrm{sp}_8(-Q)\right)^\top,$$

with $P \in [\max\{P_{\min}, W_i\}, P_{\text{tech}}]$ and $A \in [A_{\min}, A_{\max}]$, where $P_{\min}$ is the computational price floor. Within this residual-based branch, inner candidates are ranked by the residual norm, with an additional $1000 + |Q|$ when $Q < 0$. The pre-check evaluates demand at the lowest admissible price and maximum promotion:

$$Q_i^{\text{pre}} = q_0 - b_p \max\{P_{\min}, W_i\} + b_A A_{\max} + b_E E_i + b_G G_i + b_R R_i.$$

A node is classified as economically infeasible if $Q_i^{\text{pre}} < -10^{-8}$. Success requires the derivative checks below, $Q_i \geq -10^{-6}$, and no pre-check infeasibility. For each bounded variable, the utility derivative must be approximately zero in the interior, nonpositive at a lower bound, or nonnegative at an upper bound within the specified tolerance. The inner exit flag is recorded but a positive flag is not required by this success test. No explicit multiplier for the demand constraint is recovered; these checks are bound-adjusted stationarity and feasibility diagnostics, not a complete generic KKT test at an active demand boundary. The loose P_{tech} bound is checked ex post. The direct constrained SQP branches in Section 5.4.1 use separate constraint, multiplier, and positive-exit success checks.

For the finite-k branches, the positive-part term is approximated by

$$[\Delta\Pi_i]^+ \approx S_\pi \, \text{sp}_k\left(\frac{\Delta\Pi_i}{S_\pi}\right), \qquad \text{sp}_k(z) = \frac{1}{k}\ln(1 + e^{kz}). \tag{20}$$

The scale S_π is calibrated once on the no-penalty benchmark path in normalized monetary units and fixed across scenarios. In the reported experiments, $S_\pi = 8.335937$. With $\langle y_i \rangle_N = (N+1)^{-1} \sum_{i=0}^{N} y_i$, the outer objective is

$$\begin{aligned} \mathcal{L}(\theta) = &- J_m^h(\theta) + \Omega_{\text{KKT}} \langle \kappa_i^2 \rangle_N + \Omega_{\text{fail}}(1 - R_{\text{succ}}) + \Omega_Q \langle \text{sp}_{k_d}(-Q_i)^2 \rangle_N \\ &+ \Omega_X \left\langle \text{sp}_{k_d}(-G_i)^2 + \text{sp}_{k_d}(-R_i)^2 \right\rangle_N + \Omega_P \langle \text{sp}_{k_d}(P_i - 0.98 P_{\text{tech}})^2 \rangle_N. \end{aligned} \tag{21}$$

For the residual-based branch, κ_i is the norm of the bound-adjusted stationarity violations above. For the direct constrained branches, it is the Lagrangian-stationarity two-norm over the inner variables, not the combined feasibility, complementarity, and dual residual. The penalty terms are numerical safeguards, not economic costs. No boundary penalty is imposed on $E(t)$. The penalty ratio

$$R_{\text{pen}} = \frac{\mathcal{L}(\theta) + J_m^h(\theta)}{|J_m^h(\theta)| + \varepsilon_{\text{obj}}}$$

is used to verify that a reported path is not dominated by numerical penalties. For the contract diagnostic, $\mu_G(t_i)$ and $\mu_R(t_i)$ are reconstructed along the integrated reference by a backward-Euler recursion for the continuous-time costate equations, with zero terminal values. This diagnostic is not an exact discrete adjoint of the RK4 control-parameterization problem.

4.4. Multi-start selection rule

The non-convex Chapter 5 outer problem uses seven deterministic starts without early stopping to minimize Eq (21), with shared penalties and selection gates across residual-based and direct constrained runs. Their inner stationarity and success diagnostics retain the branch-specific meanings in Sections 4.3 and 5.4.1. A candidate passes the selection feasibility test when its outer objective is finite, its exit flag is not the exception flag -999, the inner success rate is at least 0.99, the

infeasibility rate is at most 0.01, and minimum demand is at least -10^{-5}. Its selection score is then the outer objective. Otherwise, the score adds $10^6 + 10^5(1 - R_{\text{succ}}) + 10^5 R_{\text{infeas}}$, where R_{infeas} is the infeasible-node fraction. The minimum-score candidate is selected; this fallback penalizes failed diagnostics rather than guaranteeing exclusion. All reported selected Chapter 5 paths have full inner success, zero infeasibility, and negligible objective penalties, making selection consistent with the highest manufacturer payoff among the tested feasible numerical candidates. Other residual, constraint-hit, instability, and penalty diagnostics are reported as checks, not all as explicit selection gates. Neither positive outer convergence flags nor global optimality are established by this rule.

Diagnostic evidence levels. Feasibility, retailer pointwise response optimality, and manufacturer outer stationarity are distinct. Proposition 1 concerns only the retailer problem under fixed leader decisions and states. Bound-adjusted residuals in residual-based runs and constraint/multiplier checks in direct runs assess that lower-level response (Section 5.4.1). Feasibility and agreement across deterministic starts do not establish outer stationarity; saved outer exit flags and native first-order measures are reported separately. A positive exit flag or an emission-bound hit alone does not certify leader optimality.

Analytical versus numerical scope. Proposition 1 gives uniqueness of the smoothed pointwise retailer response, and Proposition 2 gives the exact-hinge activated-branch representation on the original feasible set. The Softplus utility bound and contract accounting/participation identities are analytical statements under their stated conditions. In contrast, the carbon-price regime pattern, wholesale-concession magnitudes and persistence, selected exact-hinge leader paths, and C3 proximity to the integrated reference are numerical findings conditional on the control family, grids, starts, smoothing specification where applicable, and tolerances. They are not general comparative-static, global-optimality, or exact-coordination theorems.

5. Numerical simulation and case analysis

5.1. Parameter settings and numerical experiment design

For the experiments, we examine carbon-policy transmission through profit allocation and retailer disadvantageous inequity aversion. In Chapter 5, we share the economic model structure, six-parameter W/E representation, time grid, RK4 stage updates, and outer penalty/selection framework of Section 4.4. Inner objectives, tolerances, success tests, and stationarity diagnostics differ between the residual-based experiments and the direct constrained branches of Section 5.4.1.

The baseline market parameters are $q_0 = 75$, $b_p = 0.85$, $b_A = 0.75$, $b_E = 0.95$, $b_G = 0.35$, and $b_R = 0.40$. For the state dynamics, $\rho_{GE} = 0.70$, $\rho_{GA} = 0.60$, $\rho_{RE} = 0.65$, $\delta_G = 0.36$, and $\delta_R = 0.28$, with initial states $G(0) = 18$ and $R(0) = 14$. The cost and carbon-trading parameters are $c_m = 14$, $\eta_m = 1.40$, $\eta_r = 5.50$, $e_{\text{unit}} = 0.22$, $C_{\text{cap}} = 9.0$, $\phi_E = 0.45$, and the baseline carbon price $p_c = 1.10$.

For behavioral parameters, the standard channel profit-comparison coefficient is $\omega_\pi = 1.25$, and the standard baseline inequity-aversion coefficient is $\lambda_L = 1.20$. The case $\lambda_L = 1.00$ removes the additional inequity-aversion penalty, whereas $\lambda_L > 1$ represents stronger disadvantageous inequity aversion.

The planning horizon is $T = 10$, and the grid contains $N = 100$ intervals. The control bounds are $E(t) \in [0, 8]$ and $A(t) \in [0, 25]$. A loose technical upper bound $P_{\text{tech}} = 300$ is imposed only to prevent

abnormal price drift during nonlinear search; it is not an economic price cap and is checked ex post through the price-bound hit rate and the corresponding KKT residual.

The baseline behavioral Softplus parameter is $k = 8$. The scale $S_\pi = 8.335937$ is calibrated once from the no-penalty benchmark and held fixed across the carbon-price, inequity-aversion, smoothing, and contract-validation scenarios. Computational profit flows, relative profit gaps, transfers, and their discounted payoffs use normalized monetary units after division by $S_{\text{rep}} = 100$; S_π is calibrated in those same units. The tables retain that normalization. Prices, effort levels, states, and demand are not divided by S_{rep}.

The numerical experiments are organized into two parameter environments. The standard setting uses $\omega_\pi = 1.25$ and $\lambda_L = 1.20$ and is used for the carbon-price analysis with $p_c \in \{0.50, 1.10, 2.00\}$. To assess whether the baseline carbon-price result is driven by the emission-effort upper bound, in Section 5.3, we also use a preselected structural grid $\eta_m \in \{1.4, 10, 14\} \times p_c \in \{0.50, 1.10, 2.00\}$. The three cost levels represent the baseline saturated regime, an interior moderate-cost regime, and a deeper interior higher-cost regime; they were frozen before the new $p_c = 0.50$ and 2.00 outcomes were inspected. The high-pressure setting uses $\omega_\pi = 2.20$, $c_m = 14$, and $p_c = 1.10$. Under this setting, $\lambda_L \in \{1.00, 1.20, 1.50\}$ is used for inequity-aversion intensity analysis, and $k \in \{4, 6, 8, 10, 12, 14, 16\}$ is used for smoothing-parameter sensitivity with $\lambda_L = 1.50$. The standard setting first establishes how carbon-policy changes are transmitted through vertical profit allocation under moderate behavioral pressure and then tests whether that transmission changes between saturated and interior emission-effort regimes. The high-pressure setting deliberately amplifies channel profit-comparison pressure to expose the concession mechanism near the inequity kink and to stress-test the smoothing approximation. In Section 6, we evaluate the same contract logic against the two resulting decentralized benchmarks. The two environments are therefore complementary stages of one mechanism sequence–policy transmission, behavioral stress, and coordination response–rather than two interchangeable calibrations. Their cross-environment differences do not identify the causal effect of ω_π alone.

The numerical parameters are not calibrated from a specific firm-level dataset. They are specified for illustrative and mechanism-oriented analysis, with reference to common settings in low-carbon supply chain differential games, dynamic goodwill models, and behavioral supply chain studies. The baseline parameter values are summarized in Table 2.

5.2. Baseline path and diagnostic validity

In this section, we report the baseline path under the standard channel profit-comparison setting, defined by $p_c = 1.10$, $\lambda_L = 1.20$, $\omega_\pi = 1.25$, and $k = 8$. Our purpose is to establish a feasible reference path under the standard setting, rather than to draw conclusions from a single operating point.

The numerical diagnostics show that the baseline path is economically feasible and numerically stable. The retailer's inner response succeeds at all time nodes, the transaction infeasibility and numerical instability rates are zero, the bound-adjusted stationarity residuals are at the numerical tolerance level, and the loose technical price bound is not active. These checks support economic feasibility and the retailer response on the selected path; they do not establish manufacturer outer stationarity.

Under the baseline setting, emission-reduction effort reaches its upper bound, $\overline{E} = 8.000$. The average relative profit gap is $\overline{\Delta\Pi} = 3.168$, and the activation rate is 100%. The baseline discounted payoffs are

$$J_m = 77.571, \qquad J_r = 69.561, \qquad J_{SC} = 147.13.$$

These values define the standard decentralized benchmark used in the coordination analysis in Section 6.

Overall, the baseline path confirms that persistent disadvantageous inequity does not necessarily cause transaction infeasibility. Instead, the channel can still form a feasible decentralized operating path, which serves as the standard-setting anchor for carbon-price shocks and as a contrast for the stronger behavioral pressure studied later.

Table 2. Baseline parameter settings.

Category	Symbol and description	Value
Market	q_0, potential market size	75
Market	b_p, price sensitivity coefficient	0.85
Market	b_A, effect of promotional effort on demand	0.75
Market	b_E, effect of emission-reduction effort on demand	0.95
Market	b_G, effect of low-carbon goodwill on demand	0.35
Market	b_R, effect of product-specific low-carbon awareness on demand	0.40
Cost/carbon	c_m, manufacturer's unit production cost	14
Cost/carbon	p_c, baseline carbon trading price	1.10
Cost/carbon	e_{unit}, unit carbon emission coefficient	0.22
Cost/carbon	C_{cap}, carbon quota	9.0
Cost/carbon	ϕ_E, emission-offset coefficient	0.45
Cost/carbon	η_m, emission-reduction cost coefficient	1.40
Cost/carbon	η_r, promotion cost coefficient	5.50
State	ρ_{GE}, effect of emission reduction on goodwill	0.70
State	ρ_{GA}, effect of promotion on goodwill	0.60
State	δ_G, decay rate of low-carbon goodwill	0.36
State	ρ_{RE}, effect of emission reduction on the awareness state	0.65
State	δ_R, decay rate of the awareness state	0.28
Behavioral	ω_π, channel profit-comparison coefficient	1.25 / 2.20
Behavioral	λ_L, standard baseline inequity-aversion coefficient	1.20
System	ρ, discount rate	0.03
Initial states	$G(0)$, initial low-carbon goodwill	18
Initial states	$R(0)$, initial product-specific low-carbon awareness	14
Numerical	T, N, horizon and number of intervals	10, 100
Control bounds	$E(t)$, emission-reduction effort bounds	$[0, 8]$
Control bounds	$A(t)$, promotional effort bounds	$[0, 25]$
Numerical	k, baseline behavioral Softplus parameter	8
Numerical	S_π, fixed Softplus profit scale	8.335937
Numerical	P_{tech}, loose technical price upper bound	300
Numerical	S_{rep}, monetary normalization scale	100

*Note: The standard setting uses $\omega_\pi = 1.25$ and $\lambda_L = 1.20$. The high-pressure setting uses $\omega_\pi = 2.20$. Monetary indicators are scaled by $S_{\text{rep}} = 100$, while prices, effort levels, state variables, and demand are not scaled. The Softplus scale S_π is calibrated once from normalized no-penalty benchmark profits and then fixed across all numerical experiments.

5.3. Channel profit structure and inequity pressure response under carbon price shocks

In this section, we examine carbon-price shocks under the standard channel profit-comparison setting. The parameters $c_m = 14$, $\lambda_L = 1.20$, $\omega_\pi = 1.25$, and $k = 8$ are fixed, while $p_c \in \{0.50, 1.10, 2.00\}$ represents low, baseline, and high carbon price levels.

Ordinary reported path averages are arithmetic means over the 101 nodes $t_i = 0.1i$, $i = 0, \dots, 100$, with $N = 100$:

$$\overline{Y} = \overline{Y}_N = \frac{1}{N+1}\sum_{i=0}^{N} Y(t_i), \qquad \gamma_N = \frac{1}{N+1}\sum_{i=0}^{N} \mathbf{1}\{\Delta\Pi(t_i) > 0\}.$$

Activation is the fraction of nodes with a strictly positive gap. These summaries are not trapezoidal time averages. Discounted J_m, J_r, and J_{SC} use $\text{trapz}(t, e^{-\rho t}\pi)$ as in Section 4.2. Payoff differences, efficiency ratios, improvement rates, and transfer quantities are calculated from the highest available full-precision inputs and rounded once for display. In all three carbon-price scenarios, the inner response success rate

is 100%, and the transaction infeasibility and numerical instability rates are zero. Table 3 reports the main transmission variables, profit allocation, relative profit gap, and inequity activation.

Table 3. Strategic responses, profit allocation, and inequity pressure under carbon price shocks.

p_c	$\overline{W}$	$\overline{E}$	$\overline{P}$	$\overline{A}$	$\overline{Q}$	$\overline{\pi}_m$	$\overline{\pi}_r$	$\overline{\Delta\Pi}$	Act.
0.50	53.304	8.000	89.129	3.819	23.807	8.946	8.130	3.052	100%
1.10	53.503	8.000	89.240	3.801	23.691	8.992	8.071	3.168	100%
2.00	53.777	8.000	89.390	3.776	23.534	9.062	7.991	3.336	100%

*Note: Barred variables are arithmetic means over 101 grid nodes. Profits and $\overline{\Delta\Pi}$ are scaled by $S_{\text{rep}} = 100$; prices, effort levels, and demand are not scaled. Act. denotes the share of time nodes satisfying $\Delta\Pi(t) > 0$.

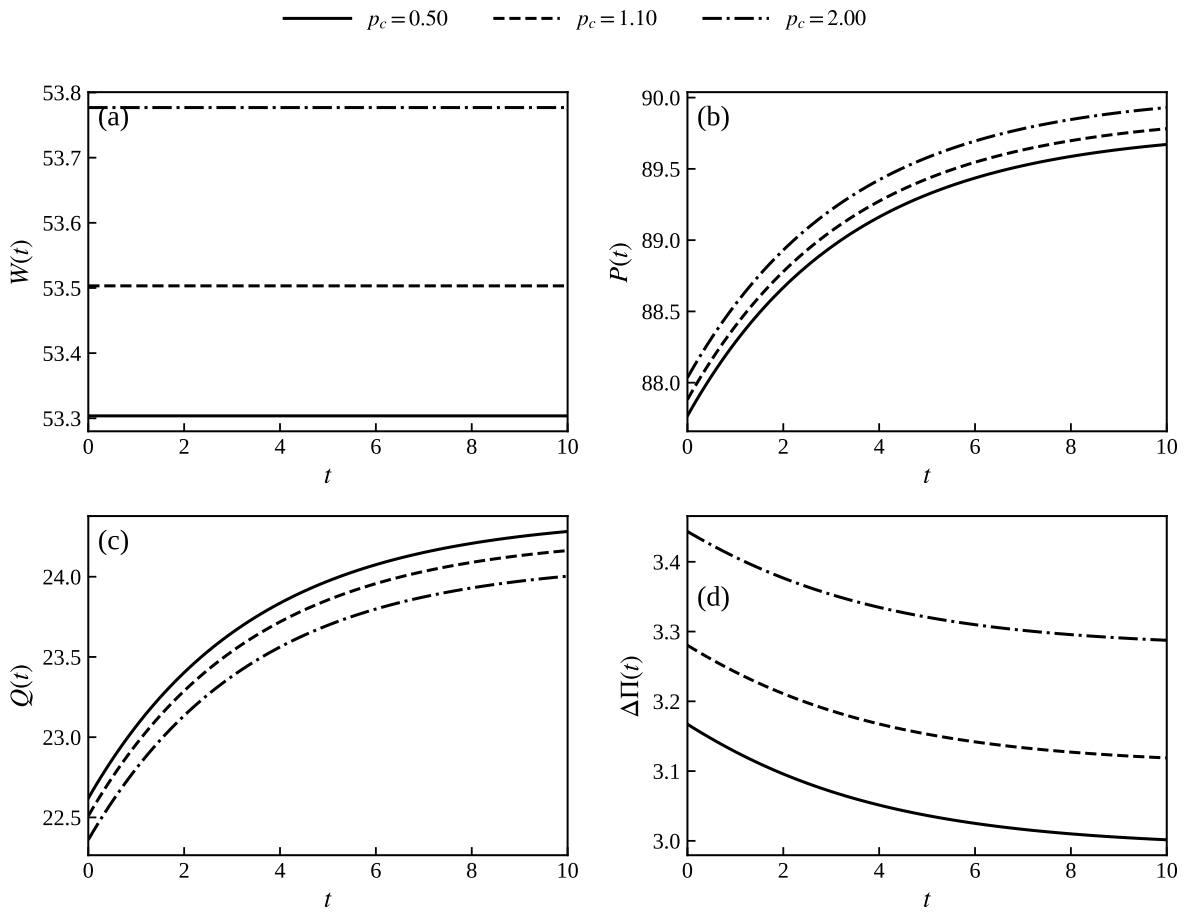


Figure 1. Dynamic paths under carbon-price sensitivity in the standard channel profit-comparison setting. Panels report $W(t)$, $P(t)$, $Q(t)$, and $\Delta\Pi(t)$ for $p_c = 0.50$, 1.10, and 2.00. Since emission-reduction effort remains saturated at its upper bound across the sampled carbon prices, carbon-price shocks mainly affect price transmission, demand, and profit allocation rather than additional marginal emission-reduction effort.

As shown in Table 3 and Figure 1, emission-reduction effort remains saturated at the upper bound across all sampled carbon prices. Carbon-price shocks therefore mainly affect price transmission, demand, and profit allocation rather than additional marginal emission-reduction effort. In particular,

a higher p_c slightly increases wholesale and retail prices, reduces demand, and raises the perceived inequity gap.

The results show that emission-reduction effort reaches its upper bound in all three carbon-price scenarios, with $\overline{E} = 8.000$. Hence, within this parameter range, carbon-price shocks no longer operate through marginal changes in emission-reduction effort. Their main effects are transmitted through price adjustment, demand, and profit allocation.

As p_c increases from 0.50 to 2.00, $\overline{W}$ rises from 53.304 to 53.777, $\overline{P}$ rises from 89.129 to 89.390, and $\overline{Q}$ falls from 23.807 to 23.534. Moreover, $\overline{\pi}_m$ increases from 8.946 to 9.062, whereas $\overline{\pi}_r$ decreases from 8.130 to 7.991. The average channel profit remains nearly stable, with only a slight decline from 17.076 to 17.053. Thus, the main effect is redistribution toward the manufacturer rather than a substantial change in total channel profit.

The perceived relative profit gap increases monotonically from 3.052 to 3.336, and the activation rate remains 100% in all three scenarios. Therefore, a higher carbon price does not mitigate the retailer's perceived disadvantageous inequity in the baseline low-cost setting. Because emission effort is saturated, the observed adjustment is transmitted mainly through wholesale and retail prices, demand, and vertical profit allocation. This baseline result is conditional on the active upper bound and is not interpreted as a general claim that carbon prices do not affect emission-reduction effort.

5.3.1. Structural robustness across emission-reduction cost regimes

To test that boundary dependence directly, the carbon-price experiment is repeated on the frozen grid

$$\eta_m \in \{1.4, 10, 14\}, \qquad p_c \in \{0.50, 1.10, 2.00\},$$

while retaining the standard behavioral setting $\omega_\pi = 1.25$, $\lambda_L = 1.20$, and $k = 8$. The cost levels were selected before the new low- and high-carbon-price cells were observed. At $p_c = 1.10$, $\eta_m = 1.4$ reproduces the baseline upper-bound regime, $\eta_m = 10$ gives a clearly interior moderate-cost path, and $\eta_m = 14$ gives a deeper interior path. A numerically sensitive transition region found in scouting around $\eta_m \in [4, 4.5]$ is deliberately excluded from the reported grid; no exact transition threshold is claimed.

Table 4. Structural robustness of carbon-price transmission across emission-reduction cost regimes.

η_m	p_c	Regime	$\overline{E}$	$\overline{W}$	$\overline{P}$	$\overline{A}$	$\overline{Q}$	$\overline{\Delta\Pi}$	Act.
1.4	0.50	Upper	8.000	53.304	89.129	3.819	23.807	3.052	100%
1.4	1.10	Upper	8.000	53.503	89.240	3.801	23.691	3.168	100%
1.4	2.00	Upper	8.000	53.777	89.390	3.776	23.534	3.336	100%
10	0.50	Interior	5.236	48.479	82.373	3.927	24.476	0.886	80.20%
10	1.10	Interior	5.216	48.640	82.474	3.902	24.322	0.986	82.18%
10	2.00	Interior	5.180	48.896	82.627	3.863	24.077	1.143	86.14%
14	0.50	Interior	3.311	47.550	79.572	3.577	22.294	1.569	100%
14	1.10	Interior	3.293	47.752	79.684	3.549	22.124	1.678	100%
14	2.00	Interior	3.266	48.060	79.851	3.509	21.870	1.842	100%

*Note: Each cell uses the same seven deterministic starts and the unchanged feasibility/selection rule. The $\eta_m = 1.4$ row reproduces the baseline Chapter 5 carbon-price results at full precision. "Upper" denotes an emission path at $E_{\max} = 8$ at all 101 nodes; "Interior" is the predeclared numerical regime classification. Barred variables are 101-node arithmetic means; Act. is the strict positive-gap node fraction. All selected cells have clean retailer responses and negligible numerical penalties. The selected interior regime is recovered by six clean same-regime starts in every $\eta_m = 10$ and 14 cell; no near-tied distinct-regime solution occurs under the frozen criterion.

Table 4 separates the saturated and interior transmission channels. The low-cost row remains at $E_{\max}$ for every sampled carbon price and exactly reproduces the baseline statistics. Once η_m is raised to 10

or 14, the selected emission paths are interior at all three price levels, so carbon-price changes are no longer mechanically blocked by the effort upper bound.

Within both tested interior regimes, the mean emission effort decreases modestly as p_c rises. For $\eta_m = 10$,

$$\overline{E} : 5.236 \rightarrow 5.216 \rightarrow 5.180,$$

and for $\eta_m = 14$,

$$\overline{E} : 3.311 \rightarrow 3.293 \rightarrow 3.266.$$

Within this grid, interior mean effort does not increase monotonically with carbon price. The selected paths reflect joint re-optimization of wholesale price, downstream response, state trajectories, and carbon-accounting terms. The evidence covers three carbon prices and three preselected cost regimes; a change in mean effort does not imply the same direction at every node. In Section 4.4, we give the broader numerical scope.

Several price-allocation responses are more persistent across regimes. At $\eta_m = 10$ and 14, increasing p_c raises $\overline{W}$ and $\overline{P}$, lowers $\overline{A}$ and $\overline{Q}$, increases the manufacturer's average profit, decreases the retailer's average profit, and enlarges $\overline{\Delta\Pi}$. At $\eta_m = 10$, the strict activation share also rises from 80.20% to 86.14%; at $\eta_m = 14$, it remains 100%. Hence, the policy–behavior transmission through vertical profit allocation is observed not only on the saturated baseline path but also in the tested interior-effort regimes.

The nine selected cells are feasible numerical candidates under the unchanged clipped-exponential control family. All seven starts are retained in each cell. The saturated row has seven clean same-regime supporters, whereas each interior cell has six; the remaining clean start reaches an inferior upper-bound candidate, and no structurally distinct path is near-tied in manufacturer payoff under the frozen criterion. Same regime does not mean identical path amplitudes. At $\eta_m = 10$ and $p_c = 0.50$, the six same-regime candidates have an $\overline{E}$ range of 0.1182839173 and a J_m range of 0.0740517409, compared with the selected $\overline{E}$ decrease of 0.0558349165 from $p_c = 0.50$ to 2.00. Pairing the six interior starts by their identical initial parameter vectors across carbon prices shows a decrease in mean effort in both price steps for every pair. At $\eta_m = 14$, the largest within-cell $\overline{E}$ range across the three prices is only 6.8868×10^{-7}, and all six paired interior starts again decrease in both steps. These saved-start ranges are neither confidence intervals nor standard errors. They support the tested regime classification and paired direction, rather than identical paths or precise repeatability of response magnitudes. The three saturated selected candidates have outer exit flag 1 and native first-order measures between 3.85×10^{-10} and 2.79×10^{-9}; the six interior selected candidates have exit flag 2 and measures between 1.99×10^{-8} and 8.22×10^{-7}. These are parameter-space termination diagnostics, not functional boundary KKT certificates. Interpretation follows Section 4.4. In Section 7.2, we discuss threshold and extrapolation limits.

5.4. Inequity-aversion intensity and smoothing sensitivity under high channel profit-comparison pressure

In this section, we investigate the high channel profit-comparison pressure setting with $\omega_\pi = 2.20$, $c_m = 14$, and $p_c = 1.10$. Following the policy-transmission analysis in Section 5.3, this stress test examines how stronger profit-comparison pressure changes the concession mechanism near the inequity kink. It does not isolate an effect of ω_π through a direct comparison with the standard scenarios. The analysis first varies $\lambda_L \in \{1.00, 1.20, 1.50\}$ under $k = 8$, and then varies $k \in \{4, 6, 8, 10, 12, 14, 16\}$ under $\lambda_L = 1.50$.

When $\lambda_L = 1.00$, the coefficient of the inequity-aversion penalty is zero, so this row serves as a reference path without an additional behavioral penalty. As λ_L increases, the retailer becomes more

sensitive to disadvantageous relative profit gaps, and the manufacturer adjusts its wholesale-price path preemptively. Table 5 reports the corresponding strategic responses, and Figure 2 shows the associated dynamic paths.

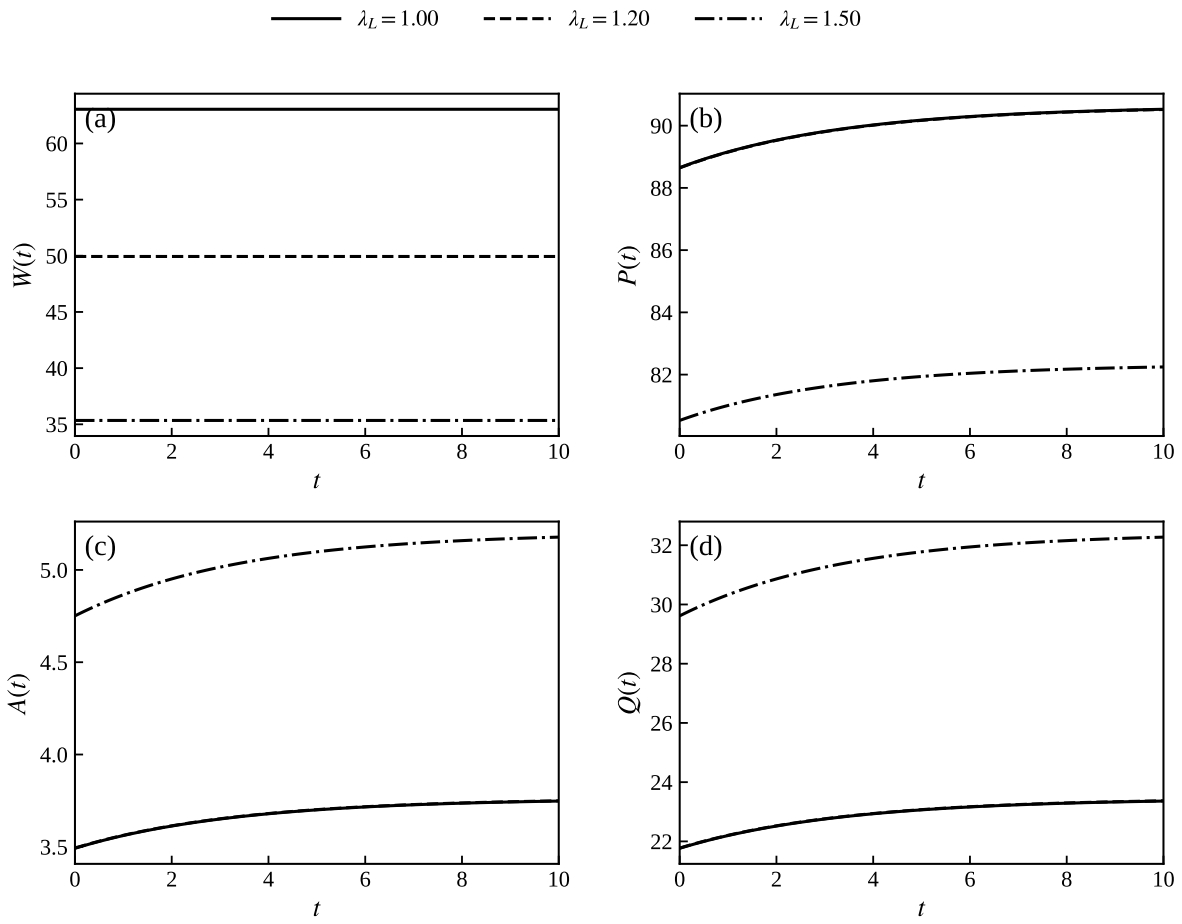


Figure 2. Dynamic paths under inequity-aversion intensity sensitivity in the high channel profit-comparison setting. Panels report $W(t)$, $P(t)$, $A(t)$, and $Q(t)$ for $\lambda_L = 1.00$, 1.20, and 1.50. A higher λ_L induces stronger preemptive wholesale-price concessions, as shown in panel (a). Between $\lambda_L = 1.00$ and $\lambda_L = 1.20$, the downstream paths of $P(t)$, $A(t)$, and $Q(t)$ remain nearly unchanged, indicating that the concession mainly reallocates channel profit through $W(t)$, consistent with the exact-hinge mechanism illustrated by Proposition 2. When $\lambda_L = 1.50$, the system approaches the inequity-aversion kink, leading to a marked reduction in retail price and a substantial expansion of promotion and demand.

The simulations illustrate a preemptive concession response in this model, consistent with established fairness-channel pricing logic [8]. As λ_L increases from 1.00 to 1.50, $\overline{W}$ decreases from 63.043 to 35.344, and $\overline{\Delta\Pi}$ falls from 18.108 to 0.019. The system remains fully activated at $\lambda_L = 1.00$ and 1.20, while the activation rate falls to 43.56% at $\lambda_L = 1.50$. Thus, the transition from a deeply activated region to a near-kink region occurs between $\lambda_L = 1.20$ and $\lambda_L = 1.50$.

The retailer-side response is expansionary. The average retail price decreases from 89.991 to 81.767, promotional effort increases from 3.675 to 5.055, and demand expands from 22.905 to 31.513. The

manufacturer's average profit falls from 10.869 to 6.340, whereas the retailer's average profit rises from 5.803 to 13.929. Hence, the decentralized response mitigates perceived inequity pressure through substantial upstream profit compression and downstream margin expansion.

Table 5. Strategic responses and profit allocation under different inequity-aversion intensities.

λ_L	$\overline{W}$	$\overline{E}$	$\overline{P}$	$\overline{A}$	$\overline{Q}$	$\overline{\pi}_m$	$\overline{\pi}_r$	$\overline{\pi}_{SC}$	$\overline{\Delta\Pi}$	Act.
1.00	63.043	8.000	89.991	3.675	22.905	10.869	5.803	16.672	18.108	100%
1.20	49.940	8.000	89.983	3.676	22.913	7.870	8.806	16.676	8.509	100%
1.50	35.344	8.000	81.767	5.055	31.513	6.340	13.929	20.269	0.019	43.56%

*Note: Barred variables are arithmetic means over 101 grid nodes under $\omega_\pi = 2.20$, $p_c = 1.10$, $c_m = 14$, and $k = 8$. Profits and $\overline{\Delta\Pi}$ are scaled by $S_{\text{rep}} = 100$. For all rows, the inner response success rate is 100%, and both infeasibility and instability rates are zero.

The branch-local transformation below follows the fairness-adjusted channel-pricing logic of Cui et al. [8], specifically their disadvantageous-inequity branch. Proposition 2 states its model-specific representation with carbon-adjusted marginal cost and promotion, retaining the original feasible set. Its role is to interpret the concession response within the surrounding dynamic low-carbon model; it does not attribute that model's state dynamics or emission decisions to Cui et al.

Proposition 2 (Effective wholesale-price equivalence)**.** *Let* $\bar{c} = c_m + p_c e_{\text{unit}}$ *and*

$$a_{\lambda,\omega} = \frac{(\lambda_L - 1)\omega_\pi}{\lambda_L}.$$

For the exact positive-part utility in Eq (8)*, within the activated branch* $\Delta\Pi(t) > 0$*, the retailer's pointwise response is locally equivalent to material-profit optimization on the original feasible set with the effective wholesale price*

$$\widetilde{W} = W + a_{\lambda,\omega}(W - \bar{c}). \tag{22}$$

Therefore, to maintain a target effective wholesale price $\widetilde{W}^*$*, the actual wholesale price must satisfy*

$$W^*(\lambda_L, \omega_\pi) = \frac{\widetilde{W}^* + a_{\lambda,\omega}\bar{c}}{1 + a_{\lambda,\omega}}. \tag{23}$$

This equivalence concerns the retailer's pointwise objective within the activated branch. The original feasibility constraint remains $P \geq W$*, not* $P \geq \widetilde{W}$*. Eqs* (22)–(23) *do not characterize the manufacturer's full intertemporal equilibrium, even if* $E(t) = E_{\max}$*; the leader's response and state dynamics still require separate analysis.*

Proof. In the activated region, the retailer's local utility can be written as

$$U_r = \lambda_L \pi_r - (\lambda_L - 1)\omega_\pi \pi_m.$$

Substituting $\pi_r = (P - W)Q - \eta_r A^2/2$, $\pi_m = (W - \bar{c})Q +$ terms independent of P and A, and $Q = q_0 - b_p P + b_A A + b_E E + b_G G + b_R R$, the retailer's pricing stationarity condition reduces to

$$Q - b_p(P - \widetilde{W}) = 0,$$

and the promotional-effort stationarity condition reduces to

$$b_A(P - \widetilde{W}) - \eta_r A = 0.$$

Thus, both stationarity conditions coincide with those of a material-profit retailer facing $\widetilde{W}$, while the feasibility constraints remain unchanged. Solving Eq (22) for W gives Eq (23).

For finite-k Softplus, the local utility derivative is

$$\nabla U_r^s = [1 + (\lambda_L - 1)\sigma]\nabla\pi_r - (\lambda_L - 1)\omega_\pi\sigma\nabla\pi_m, \qquad \sigma = \frac{1}{1 + e^{-k\Delta\Pi/S_\pi}}.$$

Thus, the corresponding local stationarity weight is

$$a_s = \frac{(\lambda_L - 1)\omega_\pi\sigma}{1 + (\lambda_L - 1)\sigma}.$$

It approaches $a_{\lambda,\omega}$ as σ approaches one on the activated branch. Because σ depends on the current decisions, this derivative identity is not a new fixed-coefficient objective equivalence or an exact characterization of the smoothed leader equilibrium.

Taking the $\lambda_L = 1.00$ row as the reference effective wholesale price gives $\widetilde{W}^* = 63.043$. Under $\omega_\pi = 2.20$, $\lambda_L = 1.20$, $c_m = 14$, $p_c = 1.10$, and $e_{\text{unit}} = 0.22$, we have $\bar{c} = 14.242$ and $a_{\lambda,\omega} = 0.3667$. Evaluating the antecedent-based representation in Proposition 2 gives

$$W^* = \frac{63.043 + 0.3667 \times 14.242}{1 + 0.3667} \approx 49.95,$$

which is close to $\overline{W} = 49.940$ in the $\lambda_L = 1.20$ row. This is a mechanism-consistency illustration using the analytical hinge formula and rounded inputs, not proof that the smoothed leader equilibrium is exactly given by that formula. For $\lambda_L = 1.50$, the selected path moves beyond the fully activated region and approaches the kink boundary, where $\overline{\Delta\Pi}$ is nearly zero and activation becomes partial.

Table 6 reports the smoothing-parameter sensitivity results under $\omega_\pi = 2.20$, $p_c = 1.10$, $c_m = 14$, and $\lambda_L = 1.50$.

Table 6. Smoothing-parameter sensitivity under high channel profit-comparison pressure.

k	$\overline{W}$	$\overline{E}$	$\overline{P}$	$\overline{A}$	$\overline{Q}$	$\overline{\pi}_m$	$\overline{\pi}_r$	$\overline{\pi}_{SC}$	$\overline{\Delta\Pi}$	Act.
4	40.020	8.000	86.699	4.227	26.351	6.483	11.811	18.295	2.452	100%
6	37.861	8.000	84.848	4.538	28.288	6.372	12.728	19.100	1.290	100%
8	35.344	8.000	81.767	5.055	31.513	6.340	13.929	20.269	0.019	43.56%
10	34.395	8.000	80.289	5.303	33.058	6.353	14.401	20.754	-0.426	0%
12	33.966	8.000	79.489	5.438	33.895	6.376	14.620	20.996	-0.593	0%
14	33.734	8.000	78.984	5.523	34.424	6.400	14.741	21.142	-0.660	0%
16	33.595	8.000	78.634	5.581	34.790	6.423	14.815	21.239	-0.684	0%

*Note: Only k is varied. For each k, seven starts are evaluated without early stopping and selection follows the penalized-objective/feasibility rule in Section 4.4. Barred variables are 101-node means; Act. is the positive-gap node fraction. Profits and relative profit gaps are scaled by $S_{\text{rep}} = 100$. For all rows, the inner response success rate is 100%, the transaction infeasibility rate is zero, and $E(t)$ remains at its upper bound.

The smoothing-parameter diagnostics show a continuous transition around the inequity-aversion kink. As k increases from 4 to 16, $\overline{W}$ and $\overline{P}$ decrease, while $\overline{A}$ and $\overline{Q}$ increase. Emission-reduction effort remains at its upper bound for all k, so the sensitivity to k is reflected in price transmission, downstream expansion, and the relative profit gap rather than in emission-reduction effort.

The average relative profit gap decreases monotonically from 2.452 to -0.684. The activation rate is 100% for $k = 4$ and $k = 6$, falls to 43.56% at $k = 8$, and becomes zero for $k \geq 10$. This does not imply that the concession mechanism is unstable. Rather, activation-based indicators are sensitive near the kink, where small changes in the Softplus approximation can change the share of activated time nodes. The strategy paths change smoothly, and the direction of wholesale-price concession and retailer-side expansion is preserved.

The manufacturer's average profit exhibits a mild U-shaped pattern and reaches its lowest value near $k = 8$. At a fixed gap, smaller k increases the positive Softplus approximation bias while reducing sharpness near the kink. The observed profit pattern therefore reflects re-optimization of the selected leader path as k changes, not a monotone measure of pointwise approximation error. When k is large, the selected path moves into the non-activated region, whereas the $k = 8$ path lies close to the kink. Accordingly, the payoff pattern is not interpreted as evidence that $k = 8$ is an optimal smoothing choice or that equilibrium error must decrease monotonically with k.

The multi-start diagnostics confirm the relevance of the selection rule. At $k = 16$, one starting point converges to an activated local path, but its discounted manufacturer profit is lower than that of the selected non-activated path. For these feasible paths with negligible penalties, the implemented selection score in Section 4.4 favors the higher discounted manufacturer payoff.

5.4.1. Exact-hinge benchmark for smoothing robustness

To distinguish the economic effect of the finite-k approximation from a change in the inner numerical algorithm, an exact positive-part benchmark is solved for the standard and high-pressure environments. For fixed W, E, G, R, introduce an epigraph variable z and solve

$$\max_{P,A,z} \quad \pi_r - (\lambda_L - 1)z$$

subject to

$$z \geq \Delta\Pi, \qquad z \geq 0,$$

together with the original demand, no-inverted-pricing, promotion, and technical-price constraints. For $\lambda_L > 1$, the objective strictly decreases in z, so an optimum satisfies $z = [\Delta\Pi]_+$. At $\lambda_L = 1$, P, A still uniquely maximize material profit under the stated nonempty-feasible-set and concavity conditions, while z is payoff-irrelevant and need not be unique; choosing $z = [\Delta\Pi]_+$ is a valid convention. Neither k nor S_π enters this exact utility. Equivalently, the minimization form is a convex pointwise problem, with unique optimal P, A under $2b_p\eta_r > b_A^2$. This certificate holds for fixed W, E, G, R; it establishes neither outer stationarity nor global optimality for the manufacturer.

Table 7. Softplus $k = 8$ and exact-hinge selected outcomes.

Environment	Utility	$\overline{W}$	$\overline{E}$	$\overline{P}$	$\overline{A}$	$\overline{Q}$	Act.	J_m	J_r	J_{SC}
Standard	Softplus $k = 8$	53.503	8.000	89.240	3.801	23.691	100%	77.571	69.561	147.132
Standard	Exact hinge	54.629	8.000	89.991	3.675	22.905	100%	77.137	66.623	143.760
High pressure	Softplus $k = 8$	35.344	8.000	81.767	5.055	31.513	43.56%	54.679	120.054	174.732
High pressure	Exact hinge	33.651	8.000	77.161	5.828	36.330	24.75%	58.117	128.187	186.305

*Note: Act. retains the Chapter 5 strict statistic $\#\{\Delta\Pi > 0\}/101$. Under the selected exact high-pressure candidate, however, none of the 101 nodes has $\Delta\Pi > 10^{-7}$: 53 nodes lie in $|\Delta\Pi| \leq 10^{-7}$ and 48 lie below -10^{-7}. The 25 strictly positive values are numerical residuals within the prescribed 10^{-7} kink tolerance band and should not be interpreted as economically positive activation. Payoffs use the same normalized monetary units and discounted trapezoidal integration as the main numerical results.

Before comparing the selected exact and smoothed numerical candidates, the new direct constrained inner solver is used as a numerical-method control for the original $k = 8$ Softplus model. At the two reference 101-node paths, the direct responses reproduce P, A, Q to the recorded precision. In full RK4 replay, the largest path difference is 4.79×10^{-7}, and the largest relative payoff difference is 2.22×10^{-10}. Re-optimizing the high-pressure $k = 8$ model from the same seven starts gives a

selected manufacturer-payoff difference of 2.17×10^{-10} and a maximum relative mean difference of 2.28×10^{-6} across W, E, P, A, and Q. Hence, the exact-versus-Softplus differences reported in Table 7 are not attributable merely to replacing the inner numerical method.

For each variable X, the reported path distance is the mean-normalized maximum nodewise deviation

$$d_X = \frac{\max_{0 \le i \le N} |X_i^s - X_i^e|}{\max\{1, (N+1)^{-1} \sum_{i=0}^{N} |X_i^e|\}}, \qquad N = 100.$$

Here, s and e denote the saved selected Softplus and exact candidate paths in the same environment. Payoff distances use

$$d_J = \frac{|J^s - J^e|}{\max\{1, |J^e|\}}.$$

These saved-candidate comparisons do not bound equilibrium error. Away from the kink, the exact and baseline Softplus paths are closer but remain distinct. In the standard environment, the exact path remains in the positive branch at all 101 nodes. The d_X values are 2.06% for W, 0.85% for P, and 3.50% for A and Q; the d_J values for J_m, J_r, J_{SC} are 0.56%, 4.41%, and 2.35%, respectively. Smoothing has a smaller effect here than under high pressure, but payoff differences remain non-negligible.

The high-pressure exact benchmark materially changes the near-kink path levels while preserving the main strategic direction. Using the above mean-normalized definition, the $k = 8$ d_X values are 5.03% for W, 6.29% for P, and 14.09% for A and Q; the absolute relative differences in J_m, J_r, and J_{SC} are 5.92%, 6.35%, and 6.21%. Nevertheless, the wholesale-price concession is not created by smoothing: The exact high-pressure mean wholesale price is 33.651, compared with 63.043 in the corresponding $\lambda_L = 1$ reference, and the exact wholesale-price path is lower at all 101 saved nodes. The selected exact path is supported by four clean outer starts; three additional clean starts converge to a lower-payoff fully positive candidate path, which is retained as evidence of outer non-convexity rather than discarded.

The saved outer termination diagnostics for the Softplus method-control high-pressure, exact high-pressure, and exact standard selected candidates are exit flag 2 with native first-order measures $1.0386094399 \times 10^{-5}$, 0.0125234408543, and $4.9751608643 \times 10^{-5}$, respectively. All three stopped on the step-size criterion; none of these measures meets the configured 10^{-8} optimality tolerance. They are native parameter-space first-order diagnostics, not percentage errors or payoff gaps. Feasibility, retailer pointwise KKT checks, and multi-start repeatability retain their separate evidence levels (Section 4.4); manufacturer outer stationarity is not established.

The pointwise calculation quantifies the additional finite-k penalty. At $k = 8$ in the high-pressure selected Softplus path, the theoretical pointwise utility-loss bound is 0.3611 in normalized utility units, while the realized maximum and 101-node mean are 0.3607 and 0.3395. Among the 57 strictly negative-gap nodes, the Softplus term imposes an additional penalty that is absent under the exact hinge, with conditional mean 0.3459 and maximum 0.3607. These pointwise utility differences satisfy the analytical bound; they do not bound equilibrium-path error.

Across the saved $k \in \{4, 6, 8, 10, 12, 14, 16\}$ selected candidates, all reported control and state path distances to the exact high-pressure benchmark are non-increasing as k rises. The manufacturer-payoff distance is not monotone; however, its absolute relative difference is 3.77% at $k = 4$, 5.92% at $k = 8$, and 4.70% at $k = 16$. This finite sequence establishes neither equilibrium convergence as $k \to \infty$ nor theoretical optimality of $k = 8$. The baseline regularization is retained, with the exact-hinge comparison delimiting its robust conclusions.

The exact positive-part benchmark preserves the qualitative wholesale-concession direction. Near the inequity kink, smoothing still affects activation and the magnitudes of prices, promotion, demand, and payoffs. In particular, the $k = 8$ strict activation rate of 43.56% describes the smoothed baseline rather than a smoothing-invariant branch measure. Therefore, in Section 6, we use that decentralized benchmark with this qualification.

Robustness scope. The cost/price grid and exact-hinge benchmark examine effort-bound and smoothing sensitivity under fixed demand and state parameters. In Section 7.2, we summarize the calibration limits. Marginal-cost wholesale pricing removes a positive demand-margin incentive when $b_E(P^I - \bar{c}) > 0$.

6. Composite contract coordination mechanism design and efficiency improvement analysis

6.1. Coordination difficulties under decentralized decision-making

In Section 5, we show feasible decentralized paths under cap-and-trade regulation and retailer disadvantageous inequity aversion, alongside double marginalization, promotional-effort externalities, and profit-allocation pressure. Wholesale concessions can compress the retailer's perceived disadvantageous gap but do not coordinate the channel. The C3 design combines effective marginal-cost wholesale pricing, promotion cost sharing, and back-end transfers: Removing the wholesale demand margin motivates direct emission-incentive support and participation-compatible redistribution.

Table 8 distinguishes the implementations underlying the comparison.

Table 8. Numerical implementations used in Chapters 5 and 6.

Implementation	Decisions and retailer response	State integration
Chapter 5 residual-based runs	Six exponential W/E parameters; baseline, finite-k, and cost-regime responses by bounded `lsqnonlin` residual minimization.	Controls and responses recomputed at RK4 stages.
Chapter 5 direct comparisons	Same six parameters. Constrained SQP: exact-hinge (P, A, z) epigraph; direct-Softplus (P, A).	Same RK4 stage updates.
New I	A_i, E_i at 101 nodes (202 variables); feasible maximizing P eliminated analytically at each node. No retailer subproblem; reference adopted after refinement and native confirmation.	Nodal A_i, E_i held within each RK4 step.
New C3	W^C and contract schedules fixed; three exponential E parameters independently optimized. Retailer response by direct constrained SQP; $E = 8$ is an outcome.	Nodal A_i, E_i held within each RK4 step.

*Note: All use $T = 10$, 100 intervals/101 nodes, discounted `trapz` payoffs, and arithmetic node means for ordinary path summaries. Inner objectives, tolerances, success tests, and KKT diagnostics remain branch-specific.

New I and C3 share state stepping but have different decision spaces. Saved D is imported from Chapter 5 arrays without reoptimization or state replay and is not replaced by exact-hinge results. Payoff gains relative to Saved D therefore do not isolate contract effects from implementation differences. The evidence concerns new I/C3 paths and the fixed C3 bundle, not recovered historical C3 trajectories or new comparisons of historical contract components. In Section 6.7, we report paired paths, accounting, separate material and utility participation, response diagnostics, and finite effort checks.

For the validation, we use Section 5's environments: Standard has $\omega_\pi = 1.25$, $\lambda_L = 1.20$, $p_c = 1.10$, and $k = 8$; and High pressure has $\omega_\pi = 2.20$, $\lambda_L = 1.50$, $c_m = 14$, $p_c = 1.10$, and $k = 8$. The integrated objective omits behavioral parameters, so both scenarios share I; D differs through ω_π, λ_L, and the joint

settings preclude isolating a causal effect of ω_π. C3 is tested only at $k = 8$ with inactive compensation $b = 0$; the exact-hinge exercise in Section 5.4 does not re-solve C3. The evidence remains conditional on the discretization and parameters, with scope and diagnostic limits specified in Sections 4.4 and 6.7.

6.2. Integrated decision reference model

To measure decentralized efficiency loss, in this section, we construct an integrated decision reference model. In the integrated mode, the manufacturer and the retailer are treated as a unified decision maker choosing $P^I(t)$, $A^I(t)$, and $E^I(t)$. The wholesale price is an internal transfer and does not enter integrated system profit.

The integrated demand is

$$Q^I(t) = q_0 - b_p P^I(t) + b_A A^I(t) + b_E E^I(t) + b_G G^I(t) + b_R R^I(t).$$

With $M^I(t) = e_{\text{unit}} Q^I(t) - \phi_E E^I(t)$, the instantaneous integrated system profit is

$$\pi_{SC}^I(t) = \left(P^I(t) - c_m - p_c e_{\text{unit}}\right) Q^I(t) - \frac{1}{2}\eta_m \left[E^I(t)\right]^2 - \frac{1}{2}\eta_r \left[A^I(t)\right]^2 + p_c C_{\text{cap}} + p_c \phi_E E^I(t). \quad (24)$$

Equation (24) shows that the effective unit marginal cost is

$$\bar{c} = c_m + p_c e_{\text{unit}}.$$

Accordingly, the contract wholesale price is set as

$$W^C(t) = \bar{c} = c_m + p_c e_{\text{unit}}. \quad (25)$$

This rule corrects the retailer's marginal pricing incentive, but it is not sufficient to ensure participation compatibility or emission-reduction incentive alignment.

The integrated reference problem is

$$\begin{aligned} \max_{P^I, A^I, E^I} \quad & J_{SC}^I = \int_0^T e^{-\rho t} \pi_{SC}^I(t)\, dt \\ \text{s.t.} \quad & \dot{G}^I(t) = \rho_{GE} E^I(t) + \rho_{GA} A^I(t) - \delta_G G^I(t), \\ & \dot{R}^I(t) = \rho_{RE} E^I(t) - \delta_R R^I(t), \\ & Q^I(t) \geq 0, \quad P^I(t) \leq P_{\text{tech}}, \\ & A^I(t) \in [A_{\min}, A_{\max}], \quad E^I(t) \in [E_{\min}, E_{\max}]. \end{aligned} \quad (26)$$

Here, P_{tech} is only a loose technical upper bound used to prevent abnormal price drift. The economically meaningful feasible region is determined by nonnegative demand and the control bounds.

Solving Eq (26) gives the integrated reference path $\Gamma^I = \{P^I, A^I, E^I, G^I, R^I, Q^I\}_{t\in[0,T]}$. This path is a numerical benchmark obtained under the specified parameterization, grid, and tolerances. A coordination contract is considered effective if the re-solved contract path approximates the integrated benchmark:

$$\Gamma^C \approx \Gamma^I.$$

When $E^I(t)$ reaches its upper bound, the corresponding condition is interpreted through boundary KKT conditions rather than interior first-order equalities.

6.3. Efficiency differences between decentralized and integrated decision-making

The material system payoff and efficiency loss under decentralized decision-making are

$$J_{SC}^{D} = J_{m}^{D} + J_{r}^{D}, \qquad L^{D} = \frac{J_{SC}^{I} - J_{SC}^{D}}{J_{SC}^{I}}. \tag{27}$$

Here, J_{m}^{D} and J_{r}^{D} denote discounted material payoffs. The retailer's inequity-aversion term affects its response and the induced path, but it is not counted as material system payoff.

The efficiency gap in Eq (27) comes mainly from double marginalization, promotional-effort externalities, and behavioral profit-allocation pressure. Channel profit comparison can activate disadvantageous inequity aversion when $\Delta\Pi(t) = \omega_{\pi}\pi_{m}(t) - \pi_{r}(t) > 0$. The activation rate is reported as

$$\mathcal{A}_{\Delta} = \gamma_{N} = \frac{1}{N+1}\sum_{i=0}^{N} \mathbf{1}\{\Delta\Pi(t_i) > 0\}, \qquad N = 100.$$

This diagnostic measures the share of activated time nodes, not the magnitude of the behavioral penalty.

6.4. Composite coordination contract design

The composite contract is denoted by

$$\mathcal{C} = \{W^{C}(t), s_{A}(t), \tau(t)\}, \qquad \tau(t) = b(t) - f(t),$$

where $W^{C}(t)$ is the contract wholesale price, $s_{A}(t) \in [0,1]$ is the manufacturer's cost-sharing ratio for retailer promotion, $b(t)$ is the contingent inequity-compensation flow, and $f(t)$ is the back-end contractual fee flow paid by the retailer to the manufacturer. A positive $\tau(t)$ represents a net transfer to the retailer, whereas a negative $\tau(t)$ represents a net transfer to the manufacturer. The wholesale price follows Eq (25). This clause removes the wholesale markup from the retailer's marginal pricing decision and mitigates price distortion.

Given a contract path, the pre-transfer profits are

$$\begin{aligned}
\pi_{r}^{C,0}(t) &= \left(P^{C}(t) - W^{C}(t)\right) Q^{C}(t) - \frac{1}{2}\left(1 - s_{A}(t)\right)\eta_{r}\left[A^{C}(t)\right]^{2}, \\
\pi_{m}^{C,0}(t) &= \left(W^{C}(t) - c_{m} - p_{c}e_{\text{unit}}\right) Q^{C}(t) - \frac{1}{2}\eta_{m}\left[E^{C}(t)\right]^{2} - \frac{1}{2}s_{A}(t)\eta_{r}\left[A^{C}(t)\right]^{2} \\
&\quad + p_{c}C_{\text{cap}} + p_{c}\phi_{E}E^{C}(t).
\end{aligned} \tag{28}$$

Adding the two pre-transfer profits yields the same material system-profit form as Eq (24) when the same operating path is induced.

Before contingent compensation, the contract-path relative profit gap is

$$\Delta\Pi^{C,0}(t) = \omega_{\pi}\pi_{m}^{C,0}(t) - \pi_{r}^{C,0}(t). \tag{29}$$

The contingent compensation flow $b(t) \geq 0$ directly reduces the residual pointwise disadvantageous inequity gap:

$$\begin{aligned}
\Delta\Pi^{C,b}(t) &= \omega_{\pi}\left[\pi_{m}^{C,0}(t) - b(t)\right] - \left[\pi_{r}^{C,0}(t) + b(t)\right] \\
&= \Delta\Pi^{C,0}(t) - (1 + \omega_{\pi})b(t).
\end{aligned} \tag{30}$$

Accordingly, the minimum pointwise compensation required to eliminate the residual disadvantageous inequity gap is

$$b_{\min}(t) = \frac{\max\{\Delta\Pi^{C,0}(t), 0\}}{1+\omega_\pi}. \tag{31}$$

The retailer's smoothed utility under the contract is

$$\begin{aligned} U_r^{C,s}(t) = \pi_r^{C,0}(t) + b(t) - f(t) \\ - (\lambda_L - 1) S_\pi \, \mathrm{sp}_k\left(\frac{\Delta\Pi^{C,0}(t) - (1+\omega_\pi)b(t)}{S_\pi}\right). \end{aligned} \tag{32}$$

The compensation $b(t)$ reduces the manufacturer's profit by $b(t)$ and increases the retailer's profit by the same amount, reducing the weighted gap by $(1+\omega_\pi)b(t)$. By contrast, the back-end fee $f(t)$ affects cumulative payoff allocation but is not included in the pointwise inequity-comparison argument. This separation follows a mental-accounting interpretation: Operating margins are salient in transaction-level comparison, whereas the back-end fee is settled as a horizon-level contractual account.

After transfers, the final instantaneous profits are

$$\pi_m^C(t) = \pi_m^{C,0}(t) - b(t) + f(t), \qquad \pi_r^C(t) = \pi_r^{C,0}(t) + b(t) - f(t).$$

The back-end fee flow is decomposed as

$$f(t) = f_0(t) + \Xi_E(t, E^C(t)), \qquad \Xi_E(t, E^C(t)) = \beta_E(t) E^C(t), \tag{33}$$

where $f_0(t)$ is the fixed redistribution component, and $\Xi_E(t, E^C(t))$ is the emission-incentive component. The incentive rate is calibrated along the integrated reference path as

$$\beta_E(t) = \big(P^I(t) - \bar{c}\big) b_E, \qquad \bar{c} = c_m + p_c e_{\text{unit}}. \tag{34}$$

Here, $P^I(t)$ is the retail-price path of the integrated reference solution obtained in the contract-design stage. Under $W^C(t) = \bar{c}$, the manufacturer no longer captures the operating margin generated by the demand expansion induced by emission-reduction effort. The direct demand-margin component of the system benefit of emission reduction along the integrated path is $\big(P^I(t) - \bar{c}\big) b_E$, which is used to calibrate the emission-incentive rate.

The direction of this payment is economically consistent with the back-end fee design. Since effective marginal-cost wholesale pricing shifts the operating margin from the manufacturer to the retailer, the retailer becomes the main beneficiary of the demand expansion induced by emission reduction. The emission-incentive component Ξ_E, as part of the back-end fee $f(t)$, transfers part of this direct demand-side benefit back to the manufacturer. Its role in sustaining the upper-bound effort is evaluated numerically together with the other C3 clauses.

Like $f_0(t)$, the emission-incentive component is recorded in the back-end contractual account and is not included in the retailer's pointwise inequity-comparison argument. Thus, only $b(t)$ directly reduces the residual pointwise inequity gap in Eq (30), whereas $f_0(t)$ and $\Xi_E(t, E^C(t))$ affect intertemporal payoff allocation and emission-reduction incentives. When the integrated emission-reduction path reaches its upper bound, sustaining that boundary must be assessed using the manufacturer's reduced problem and boundary/KKT conditions; the direct incentive formula alone does not establish this outcome.

6.5. Contract feasibility and participation constraints

The contract is implementable only if the induced path generates sufficient system material payoff and the transfer arrangement satisfies the participation constraints of both members. Let the discounted pre-transfer payoffs under the contract be

$$J_m^{C,0} = \int_0^T e^{-\rho t}\pi_m^{C,0}(t)\,dt, \qquad J_r^{C,0} = \int_0^T e^{-\rho t}\pi_r^{C,0}(t)\,dt.$$

The corresponding contract-generated system payoff is

$$J_{SC}^{C} = J_m^{C,0} + J_r^{C,0}.$$

Transfers do not change the total system payoff; they only redistribute payoff between the manufacturer and the retailer.

Let

$$B = \int_0^T e^{-\rho t} b(t)\,dt$$

denote the discounted contingent inequity compensation, and let

$$F = \int_0^T e^{-\rho t} f(t)\,dt = F_0 + F_E$$

denote the discounted total back-end fee, where

$$F_0 = \int_0^T e^{-\rho t} f_0(t)\,dt, \qquad F_E = \int_0^T e^{-\rho t}\Xi_E(t, E^C(t))\,dt.$$

Thus, F includes the fixed redistribution component and the emission-incentive component. The final material payoffs after transfers are

$$\tilde{J}_m^C = J_m^{C,0} - B + F, \qquad \tilde{J}_r^C = J_r^{C,0} + B - F. \tag{35}$$

The material-payoff participation constraints are

$$\tilde{J}_m^C \geq J_m^D, \qquad \tilde{J}_r^C \geq J_r^D.$$

Substituting Eq (35) gives the feasible interval for the total back-end fee:

$$J_m^D - J_m^{C,0} + B \leq F \leq J_r^{C,0} + B - J_r^D. \tag{36}$$

This interval is nonempty if

$$J_{SC}^C \geq J_{SC}^D.$$

Therefore, the contract path must generate at least as much total material payoff as the decentralized benchmark. The emission-incentive component Ξ_E affects the manufacturer's incentive and the intertemporal payoff allocation through F, but it does not change the total material payoff because it is an internal transfer.

The minimum discounted inequity compensation is

$$B_{\min} = \int_0^T e^{-\rho t} \frac{\max\{\Delta\Pi^{C,0}(t), 0\}}{1 + \omega_\pi}\, dt.$$

Additionally, if $\Delta\Pi^{C,0}(t) \le 0$ along the contract path, then $B_{\min} = 0$. This means that no compensation is needed to make the exact positive-part gap nonpositive on that path; it does not imply a zero finite-k Softplus penalty. Both reported C3 scenarios have $B_{\min} = B = 0$. The positive-b contingency is inactive there and has not been numerically validated as an active equilibrium mechanism.

The retailer's inequity-averse utility increment can be defined as a supplementary behavioral acceptability diagnostic:

$$\Delta J_r^U = J_r^{C,U} - J_r^{D,U}.$$

Material participation and behavioral-utility participation are evaluated below on the same independently optimized C3 path with the same frozen contract. Define the conditional manufacturer payoff $M_0 = J_m^{C,0} - B + F_E$, the retailer material payoff before the fixed fee $R_0 = J_r^{C,0} + B - F_E$, and the corresponding smoothed utility V_0. Here, R_0 is an accounting quantity, not the initial awareness stock. The required bounds are

$$J_m^D - M_0 \le F_0 \le R_0 - J_r^D, \qquad F_0 \le V_0 - J_r^{D,U}.$$

The predeclared equal-material-surplus rule chooses

$$F_0 = J_m^D + \tfrac{1}{2}(M_0 + R_0 - J_m^D - J_r^D) - M_0.$$

The implementation sets a constant fixed-fee flow with this discounted present value and then freezes it. Given fixed W^C, s_A, β_E, b, the fixed fee is excluded from the fairness gap, does not change the feasible set, and adds the same constant to every manufacturer operating payoff (and subtracts it from every retailer utility). Conditional operating optimization may therefore use $f_0 = 0$; the fee is not reallocated after deviations. The utility bound is checked separately and is not enforced by changing this fee rule. All reported monetary flows and present values use $S_{\text{rep}} = 100$ normalization; raw $\beta_E E$ and f_0 are divided by 100 exactly once, without assigning an empirical currency unit.

6.6. Derivation of contract-support conditions

6.6.1. Integrated-reference and retailer-side conditions

Let $\mu_G(t)$ and $\mu_R(t)$ denote the current-value costates in the analytical integrated optimal-control conditions. Along an exact interior solution, those conditions relate the operating path to its state values. The new numerical implementation instead optimizes nodal controls for a discrete problem. Backward-Euler costate reconstruction is retained only as a diagnostic along the saved reference, not as an exact state–costate solution or a certificate of discrete optimality. Promotion sharing uses retailer-FOC inversion along P^I, A^I, as distinguished below.

For interior controls and inactive nonnegative-demand constraint, the integrated first-order conditions are

$$\begin{aligned} &Q^I(t) - b_p\big(P^I(t) - \bar{c}\big) = 0, \\ &b_A\big(P^I(t) - \bar{c}\big) - \eta_r A^I(t) + \rho_{GA}\mu_G(t) = 0, \\ &b_E\big(P^I(t) - \bar{c}\big) + p_c\phi_E - \eta_m E^I(t) + \rho_{GE}\mu_G(t) + \rho_{RE}\mu_R(t) = 0. \end{aligned} \tag{37}$$

Boundary cases are interpreted through KKT complementarity. This treatment is essential because the integrated emission-reduction path reaches $E_{\max}$ in the numerical validation.

Under $W^C(t) = \bar{c}$, the following material-profit conditions describe an ideal retailer-side target when the exact-hinge penalty is locally inactive and transfers are locally fixed with respect to P and A. Merely making the residual gap zero does not remove kink effects, and a finite-k Softplus derivative generally remains nonzero at a negative gap. Accordingly, these target conditions are not asserted as exact first-order conditions of the implemented smoothed response:

$$Q^C(t) - b_p\big(P^C(t) - W^C(t)\big) = 0,$$

and

$$b_A\big(P^C(t) - W^C(t)\big) - \big(1 - s_A(t)\big)\eta_r A^C(t) = 0.$$

The pricing condition coincides with the integrated pricing condition because $W^C(t) = \bar{c}$. Comparing the promotional-effort condition with Eq (37) gives

$$s_A^*(t) = 1 - \frac{b_A[P^I(t) - \bar{c}]}{\eta_r A^I(t)} = \frac{\rho_{GA}\mu_G(t)}{\eta_r A^I(t)}. \tag{38}$$

The second equality in Eq (38) requires the exact integrated interior promotion FOC and $A^I(t) > 0$. The implementation uses only the first expression, clipped to $[0, 1]$. In the new saved terms, the share ranges from numerical zero to 0.5834092, with no clipping; the maximum absolute difference between the raw FOC-inversion and reconstructed-costate schedules is 0.2907779. This difference is not a rounding error or evidence that the two constructions are interchangeable. The costate expression remains diagnostic only.

6.6.2. Emission-incentive condition

Emission-reduction incentives require separate treatment. Effective marginal-cost wholesale pricing removes the manufacturer's wholesale markup. Although this pricing rule mitigates price distortion, it also eliminates the manufacturer's demand-side operating margin from the demand expansion induced by emission-reduction effort. Therefore, marginal-cost wholesale pricing alone may weaken the manufacturer's incentive to sustain the integrated emission-reduction level.

Under the integrated benchmark, the direct pointwise demand-margin component of the marginal benefit of emission-reduction effort is

$$b_E\big(P^I(t) - \bar{c}\big).$$

However, under $W^C(t) = \bar{c}$, the manufacturer does not capture this margin through wholesale revenue. The emission-incentive component therefore transfers this demand-side marginal benefit back to the manufacturer through the back-end fee account. Accordingly, the incentive rate is calibrated along the integrated reference path as

$$\beta_E(t) = b_E\big(P^I(t) - \bar{c}\big),$$

which is the same definition as Eq (34). Here, $P^I(t)$ is the retail-price path of the integrated reference solution obtained in the contract-design stage.

This calibration supports the direct demand-margin term $b_E(P^I - \bar{c})$. The full integrated emission condition in Eq (37) also contains $\rho_{GE}\mu_G + \rho_{RE}\mu_R$, in addition to the carbon and effort-cost terms. The

manufacturer's reduced contract problem can further include effects through the retailer's response and promotion-sharing costs. Thus, β_E alone does not establish equality of complete intertemporal marginal incentives. Under the reported parameterization, the tested C3 bundle numerically restores $E = E_{\max}$; this is a boundary outcome to be interpreted through KKT inequalities, not an interior equality or a general necessity theorem for Ξ_E.

The implemented contract schedules can be summarized as

$$\begin{aligned} W^C(t) &= \bar{c}, \\ s_A^{\text{impl}}(t) &= \text{clip}_{[0,1]}\left(1 - \frac{b_A[P^I(t) - \bar{c}]}{\eta_r A^I(t)}\right), \\ \beta_E(t) &= b_E\big(P^I(t) - \bar{c}\big). \end{aligned} \tag{39}$$

Together with the participation-compatible transfer interval and the corrected contingent compensation rule, these schedules define the tested C3 bundle. The reported $B = 0$ cases do not validate the positive-compensation contingency.

6.7. New fixed-contract validation on paired saved paths

6.7.1. Experimental design and numerical scope

Implementation details are summarized in Table 8. For the validation, we use Section 5.1's physical parameters, $S_{\text{rep}} = 100$, $S_\pi = 8.335937$, and $k = 8$. Saved D remains an imported benchmark whose historical outer-quality limitations are not upgraded by the new C3 checks.

The initial nine I starts did not meet the original 10^{-7} quality conditions. The adopted reference was subsequently obtained from the saved selected candidate through analytic-gradient refinement, one exact-Hessian active-set correction, and one native solver confirmation. Its native first-order measure is 2.78×10^{-15}; independent parameter and price KKT checks satisfy the unchanged 10^{-7} conditions. It remains a numerically qualified discrete reference, not a proven global upper bound. The refinement history and unsuccessful original records are preserved.

After adopting I, the schedules $W^C = 14.242$, s_A, and β_E are constructed once and fixed. Compensation is fixed ex ante at $b = 0$, restricting validation to the inactive-compensation branch. In each scenario, the manufacturer independently optimizes

$$E_\theta(t) = \text{clip}_{[0,8]}\{\theta_1 + \theta_2 e^{-\theta_3 t}\}, \quad \theta_1 \in [0, 8], \quad \theta_2 \in [-8, 8], \quad \theta_3 \in [0.001, 2].$$

The seven unchanged starts are $(7.8, .2, .1)$, $(8, 0, .1)$, $(6, .5, .2)$, $(4, 1, .2)$, $(2, 1, .15)$, $(1, .5, .1)$, and $(.5, .5, .1)$. SQP uses at most 2,000 outer iterations/50,000 evaluations and 300 inner iterations/1,500 evaluations, with 10^{-7} feasibility and optimality tolerances, outer step tolerance 10^{-9}, and inner step tolerance 10^{-10}. Retailer responses maximize smoothed utility under the original demand and box constraints. Selection maximizes the finite, unpenalized conditional manufacturer payoff among completed feasible starts; ties within 10^{-9} select the earlier start. Both scenarios select start 1. All 14 starts have records, but start 2 in each scenario has a first-order measure above tolerance; not all starts are claimed to be first-order qualified. Effort is optimized over its original bounds, not fixed to eight.

Coordination efficiency is reported without capping:

$$\eta_C = \frac{J_{SC}^C - J_{SC}^D}{J_{SC}^I - J_{SC}^D}. \tag{40}$$

The new saved J_{SC}^{I} and both C3 system payoffs are 202.4440672055 at the reported precision, and $\eta_C = 1$ at saved double precision. This agreement does not make the local discrete reference a theoretical upper bound.

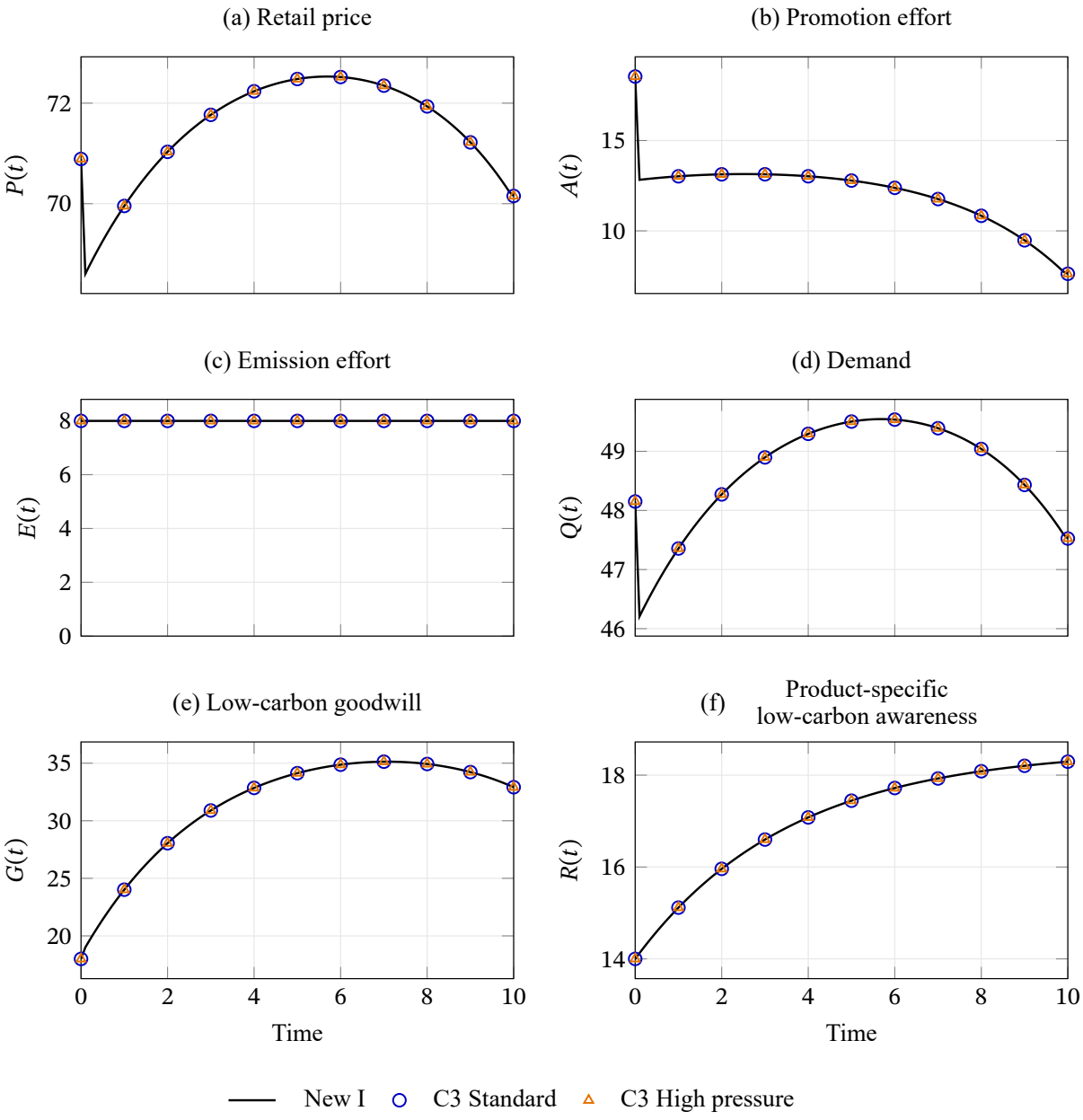


Figure 3. New integrated reference and independently selected C3 paths from complete saved arrays. Black lines show I; open circles and triangles show Standard and High-pressure C3 at every tenth node for legibility. All 101 nodes are used in the reported distances. Panels show P, A, E, Q, G, R without artificial offsets or amplified residuals; near-overlap is the actual result. Effort reaches its original upper bound as an outcome. Maximum mean-normalized node deviations over the six variables are 2.84093×10^{-8} and 4.10514×10^{-8}, respectively.

6.7.2. Paired operating paths and same-path participation

Following Sections 6.4–6.5, *payoffs*: π denotes instantaneous material profit and J its discounted cumulative counterpart; and $C, 0$ denotes pre-transfer quantities and $\tilde{J}^C$ post-transfer material payoffs. $J_r^{C,U}, J_r^{D,U}$ are discounted behavioral utilities. *Fees*: f_0, Ξ_E, f are flows; F_0, F_E, F are their discounted present values, with $F = F_0 + F_E$ the total fee, not the fixed redistribution fee. B is the compensation present value. *Pre-fee quantities and scales*: M_0 includes F_E but excludes F_0; R_0, V_0 are retailer material payoff and utility before the fixed fee. This accounting R_0 differs from the initial product-specific low-carbon awareness R_0. Monetary normalization uses $S_{\text{rep}} = 100$; the separate Softplus scale is $S_\pi = 8.335937$, in the same normalized units, without empirical currency calibration.

Table 9. Saved decentralized benchmarks and new paired I/C3 operating results.

Scenario	Mode	$\overline{P}$	$\overline{A}$	$\overline{E}$	$\overline{Q}$	J_{SC}	η_C
Standard	Saved D	89.2404	3.8006	8.0000	23.6907	147.1325	0.0000
High pressure	Saved D	81.7665	5.0555	8.0000	31.5125	174.7320	0.0000
Both	New I	71.5049	12.0314	8.0000	48.6735	202.4441	1.0000
Standard	New C3	71.5049	12.0314	8.0000	48.6735	202.4441	1.0000
High pressure	New C3	71.5049	12.0314	8.0000	48.6735	202.4441	1.0000

*Note: Separate I and C3 rows are retained even when displayed values agree. Monetary payoffs use $S_{\text{rep}} = 100$; no empirical currency calibration is asserted. D is imported with a different RK4 response convention. Efficiencies use unrounded saved values and are not capped.

Table 10. Same-path final payoffs, fixed and total fees, and separate participation checks.

Indicator	Standard	High pressure
J_m^D	77.571352	54.678540
J_r^D	69.561115	120.053505
$J_r^{D,U}$	63.996629	116.866761
M_0	21.899816	21.899816
F_0, fixed fee	83.327337	46.634735
F_E, emission incentive	37.578435	37.578435
$F = F_0 + F_E$, total fee	120.905772	84.213170
$\tilde{J}_m^C$	105.227152	68.534551
$\tilde{J}_r^C$	97.216915	133.909516
$J_r^{C,U}$	97.216915	133.909516
Manufacturer material increment	27.655800	13.856011
Retailer material increment	27.655800	13.856011
Retailer utility increment	33.220286	17.042755
System payoff gain over saved D	37.5931%	15.8597%
$B_{\min}, B$	0, 0	0, 0
Material interval for F_0	[55.671537, 110.983137]	[32.778725, 60.490746]
Utility upper bound for F_0	116.547622	63.677490
Material / utility participation	Pass / Pass	Pass / Pass
$\lvert\tilde{J}_m^C + \tilde{J}_r^C - J_{SC}^C\rvert$	0	2.84×10^{-14}

*Note: Computed from unrounded final C3 records and saved D arrays; $J_{SC}^C = 202.4440672055$. M_0 includes the emission incentive but excludes the fixed fee. The intervals constrain F_0, not F; the total-fee material interval is shifted upward by F_E. Participation tolerance is 10^{-7}, accounting tolerance 10^{-9}. The fee rule was not adjusted to secure utility participation.

Table 9 keeps the imported D paths, new I, and independently selected C3 paths separate. All barred variables are arithmetic means over the 101 saved nodes. Figure 3 is newly drawn from the complete paired arrays; the curves nearly coincide on their actual scales. Define

$$d_X = \frac{\max_i |X_i^C - X_i^I|}{(N+1)^{-1} \sum_i |X_i^I|}, \qquad X \in \{P, A, E, Q, G, R\}.$$

The largest of these six ratios is 2.84093×10^{-8} in Standard and 4.10514×10^{-8} in High pressure. These are ratios, not percentages. The predeclared 1% proximity reference is satisfied; it was not used to tune parameters or select a better-looking candidate.

Table 10 reports finalized payoffs on each selected C3 path after the equal-material-surplus rule fixes F_0 once. Moreover, material constraints and the separate post-fee behavioral-utility constraint hold. Tiny residual Softplus penalties mean that the displayed agreement of retailer material payoff and utility is not a mathematical identity.

Both final paths have inactive compensation, $B_{\min} = B = 0$, and negative pre-transfer gaps. Neither positive-compensation equilibrium nor exact-hinge C3 is validated. The imported high-pressure D path retains the near-kink qualification in Section 5.4; the C3 improvement does not imply a new D solve.

6.7.3. Response certificates and finite effort-deviation checks

Pointwise response evidence combines demand/box feasibility, a positive native exit flag, stationarity, complementarity and dual residuals, and a sufficient curvature certificate for the actual fixed cost share. The no-sharing uniqueness argument is not simply reused. Writing $g = \Delta\Pi^{C,b}$ for the normalized gap and H_r, H_m for the normalized pre-transfer profit Hessians and $H_g = \omega_\pi H_m - H_r$, the utility Hessian equals

$$H_r - (\lambda_L - 1)\sigma H_g - (\lambda_L - 1)\frac{k}{S_\pi}\sigma(1-\sigma)\nabla g \nabla g^{\top}, \quad \sigma = \frac{1}{1+e^{-kg/S_\pi}}.$$

The last term is negative semidefinite. Negative definiteness at the endpoints of the admissible σ interval is sufficient for the affine part. Moreover, where the conservative interval $[0,1]$ is insufficient, a feasible-domain upper bound on g, using $(P - \bar{c})Q \geq 0$ and the original effort/promotion boxes, gives $\sigma \leq \sigma_{\max}$. The saved endpoint tests on $[0, \sigma_{\max}]$ then certify the actual response domain under $W^C = \bar{c}, b = 0$. For the selected path and all diagnostic paths, Standard uses the conservative certificate at all 3,030 saved selected nodes; High pressure uses it at 3,000 nodes and the feasible-gap certificate at 30. These counts include repeated states. Maximum selected-node KKT residuals are 1.7603×10^{-8} and 2.2627×10^{-8}, below 10^{-7}; the original conservative failures are retained, not relabeled as successes.

For reproducibility, let $s = s_A(t)$, $\kappa = 1 - (1+\omega_\pi)s$, and define

$$E^\star = \mathrm{clip}\left(\frac{p_c\phi_E}{\eta_m}, [E_{\min}, E_{\max}]\right), \qquad C^\star = p_c C_{\mathrm{cap}} + p_c\phi_E E^\star - \frac{\eta_m}{2}(E^\star)^2.$$

Under $W^C = \bar{c}$, $b = 0$, $P \geq \bar{c}$, and $Q \geq 0$, the normalized comparison gap satisfies

$$g \leq \bar{g} = \frac{\omega_\pi C^\star + \frac{\eta_r}{2}\left[\max\{\kappa,0\}A_{\max}^2 + \min\{\kappa,0\}A_{\min}^2\right]}{S_{\mathrm{rep}}}, \qquad \sigma_{\max} = \frac{1}{1+\exp[-k\bar{g}/S_\pi]}.$$

The inequality follows because the omitted term $-(P-\bar{c})Q/S_{\mathrm{rep}}$ is nonpositive over the feasible set. Hence, the affine Hessian component $H_r - (\lambda_L - 1)\sigma H_g$ is a convex combination of its endpoint matrices for $\sigma \in [0, \sigma_{\max}]$; if both endpoints are negative definite under the stated curvature tolerance, the additional outer-product term above preserves negative definiteness. This certificate is used only when its stated assumptions hold and does not replace the numerical KKT, feasibility, complementarity, or dual checks.

The manufacturer parameter diagnostics and actual effort checks are distinct. Both selected paths lie on a complete clipping plateau. Each scenario has five available parameter perturbations, all with zero actual effort change, and one negative third-parameter direction unavailable at its lower bound. These parameter checks do not supply evidence against economic effort deviations. Separately, 24 nonzero feasible nodal deviations per scenario test a uniform shift, impulses at nodes 1, 26, 51, 76, and 101, and a linear tilt, at step fractions $10^{-4}, 10^{-3}$, and 10^{-2} of the original effort range. Directions that produce no change after clipping are omitted. The actual maximum effort changes are $0.0008, 0.008$, and 0.08. Every available deviation has its own saved retailer responses and state path under the same clauses.

All 24 effective deviations decrease manufacturer payoff. Actual changes range from -0.254891364924 to $-6.721252323 \times 10^{-6}$ in Standard and from -0.254891399079 to $-6.755451238 \times 10^{-6}$ in High pressure. The code's zero-valued best-gain accumulator is a maximum with the unperturbed baseline, not a zero-gain effective deviation. All utilized deviation responses meet the quality checks, with no unresolved effective evaluation. Diagnostics remove the same additive F_0 from the baseline and every deviation; adding the frozen fee back leaves each payoff difference unchanged within 1.43×10^{-14}. No fee is reallocated.

Table 11 summarizes the selected-candidate response and finite-direction validation.

Table 11. Selected-candidate response and finite-direction validation.

Check	Standard	High pressure
Selected start / native exit flag	1 / 1	1 / 1
Native outer first-order measure	2.9335×10^{-10}	0
Largest six-variable relative path deviation	2.84093×10^{-8}	4.10514×10^{-8}
Available parameter directions / actual E change	5 / 0	5 / 0
Effective effort directions / unresolved evaluations	24 / 0	24 / 0
Largest actual effort-deviation payoff change	-6.72125×10^{-6}	-6.75545×10^{-6}
All 11 predeclared finite checks	Pass	Pass

The 11 recorded checks cover feasibility, pointwise response, parameter diagnostics, finite effort directions, proximity, I quality, both participation criteria, accounting, inactive compensation, and reference non-exceedance. Passing them does not exhaust the 101-dimensional effort domain or continuous-time deviations, certify global optimality, or turn reported payoff equality into exact trajectory equality.

7. Conclusions and managerial implications

7.1. Main conclusions

The open-loop analysis of a manufacturer-led low-carbon channel with a myopic, inequity-averse retailer yields three conditional findings.

First, carbon-price transmission depends on the effort regime. In the tested low-cost setting, effort remains at its upper bound and adjustment occurs through prices, demand, and profit allocation. In the two higher-cost interior regimes, mean effort instead declines modestly as carbon price rises. Across the tested cost regimes, higher carbon prices raise mean wholesale and retail prices, reduce demand, shift average profit toward the manufacturer, and increase the retailer's disadvantageous profit gap. The results therefore link the emission response to the active cost/bound regime, rather than implying that carbon pricing is ineffective or always increases effort.

Second, fixed-contract C3 paths closely approach the discrete integrated reference under the stated discretization, $k = 8$, and inactive-compensation branch. Material-profit and post-fee retailer-utility participation hold under the predeclared fixed-fee allocation. In Section 6.7, we report path proximity, pointwise response checks, and effective effort deviations under frozen clauses, separately from clipping-platform diagnostics. Payoff gains are measured relative to imported D, whose implementation differs from I/C3; they cannot isolate a pure contract effect from implementation differences. Positive compensation and exact-hinge C3 remain outside the validated scope.

Third, stronger inequity aversion under high profit-comparison pressure induces preemptive wholesale-price concessions. Proposition 2 uses the established logic of Cui et al. [8] only within the exact activated branch. The exact positive-part benchmark preserves the concession direction, but near-kink activation and response magnitudes differ materially from the smoothed baseline. The $k = 8$ strict activation statistic and the exact tolerance-based partition therefore answer different questions. In Section 5.4.1, we retain the definitions and numerical comparison; the pointwise Softplus utility bound does not bound equilibrium-path error.

7.2. Managerial implications and future research directions

These implications concern stylized two-echelon, manufacturer-led channels with credible, salient low-carbon information, credible wholesale/emission commitments, relatively stable conditions, and enforceable intertemporal transfers. They are conditional lessons from a mechanism-oriented parameterization, not a universal ranking of contracts or evidence for weak-signal, highly volatile, or noncontractible settings.

Carbon pricing should be assessed jointly with emission-reduction cost, technological capacity, and vertical profit allocation. At the effort upper bound, price changes operate mainly through prices, demand, and profit allocation. Interior effort restores an emission channel, but its response need not increase monotonically, as the tested $\eta_m = 10$ and 14 cases show. Policymakers and managers should therefore assess the prevailing cost/bound regime and behavioral pressure rather than infer emission effects from carbon price alone.

Voluntary wholesale-price concessions can reduce perceived inequity and expand demand under high profit-comparison pressure, but compress manufacturer profit without necessarily internalizing promotion spillovers or ensuring system efficiency. The C3 evidence therefore motivates considering wholesale pricing, promotion sharing, direct emission-incentive support, and redistribution jointly.

Contract design should assess emission incentives and participation jointly. The C3 checks support the implemented bundle without proving that standalone instruments fail or every component is necessary. Within the intertemporal account, fixed redistribution F_0 and emission incentives F_E are distinguished from their total F. Bilateral compensation can address a positive residual gap through $1 + \omega_\pi$, but that branch was inactive and requires separate equilibrium validation.

The parameters are mechanism-oriented, and the behavioral coefficients are not empirically estimated. Product-specific low-carbon awareness responds only to observable emission-reduction information after its inherited initial stock. Public campaigns, social diffusion, intrinsic preference changes, and promotion-to-awareness spillovers are omitted; adding an exogenous inflow or promotion term could change demand persistence and policy–behavior transmission. The myopic retailer omits promotion's continuation value, whereas the manufacturer internalizes state dynamics and commits to open-loop paths. Retailer foresight could change all decision paths in directions not established here. Near-kink activation

and magnitudes depend on smoothing and the selected candidate of the non-convex leader problem. As detailed in Sections 4.4 and 5.4.1, finite-k comparisons do not prove equilibrium convergence, and some selected Chapter 5 paths fail the configured outer stationarity tolerance despite valid pointwise retailer checks. The finite C3 checks in Section 6.7 do not certify all discrete directions, function-space stationarity, or global optimality. Contract evidence remains conditional on its discretization, $k = 8$, and inactive compensation; neither an exact-hinge C3 re-solve nor a positive-compensation equilibrium is validated. The three-by-three cost/price grid does not identify a universal transition threshold. Demand sensitivities, state-accumulation coefficients, and decay rates remain fixed, so effects on timing, magnitudes, and some leader-level directions remain untested. The sensitive $\eta_m \in [4, 4.5]$ scouting region is not an exact boundary, and clipped-exponential controls restrict admissible paths. Thus, in future work, researchers may estimate behavior from experimental, survey, or transaction data; broaden awareness formation and cost/price domains; study alternative controls and nonsmooth or global leader methods; allow both members to optimize intertemporally under feedback or receding-horizon strategies; and examine platform channels, competing retailers, multiple manufacturers, stochastic demand, carbon-price uncertainty, and stochastic differential games.

Author contributions

Bo Xu: Conceptualization, supervision, methodology, validation, and writing–review and editing. Yunlong Tian: Methodology, software, formal analysis, validation, visualization, writing–original draft, and writing–review and editing. All authors have read and approved the final version of the manuscript.

Use of Generative-AI tools declaration

During the preparation of this manuscript, the authors used OpenAI's ChatGPT and Codex to assist with language editing, structural refinement, LaTeX formatting, code preparation, and consistency checks for numerical and document workflows. The authors reviewed the generated material, verified the reported results against the underlying model and saved evidence, and take full responsibility for the accuracy, integrity, and originality of the manuscript.

Acknowledgments

This research received no specific grant from any funding agency in the public, commercial, or not-for-profit sectors.

Conflict of interest

The authors declare no conflicts of interest in this paper.

References

1. S. Benjaafar, Y. Li, M. Daskin, Carbon footprint and the management of supply chains: Insights from simple models, *IEEE Trans. Autom. Sci. Eng.,* **10** (2013), 99–116. https://doi.org/10.1109/TASE.2012.2203304

2. G. Hua, T. C. E. Cheng, S. Wang, Managing carbon footprints in inventory management, *Int. J. Prod. Econ.,* **132** (2011), 178–185. https://doi.org/10.1016/j.ijpe.2011.03.024
3. S. Du, L. Zhu, L. Liang, F. Ma, Emission-dependent supply chain and environment-policy-making in the "cap-and-trade" system, *Energy Policy,* **57** (2013), 61–67. https://doi.org/10.1016/j.enpol.2012.09.042
4. S. Xu, K. Govindan, W. Wang, W. Yang, Supply chain management under cap-and-trade regulation: A literature review and research opportunities, *Int. J. Prod. Econ.,* **271** (2024), 109199. https://doi.org/10.1016/j.ijpe.2024.109199
5. M. Nerlove, K. J. Arrow, Optimal advertising policy under dynamic conditions, *Economica,* **29** (1962), 129–142. https://doi.org/10.2307/2551549
6. C. Xu, D. Zhao, B. Yuan, L. He, Differential game model on joint carbon emission reduction and low-carbon promotion in supply chains, *J. Manag. Sci. China,* **19** (2016), 53–65. https://doi.org/10.3969/j.issn.1007-9807.2016.02.005
7. Y. Wang, Q. Zhu, Long-term emission reduction decisions of a supply chain under different carbon emission permit allocation rules, *Syst. Eng. Theory Pract.,* **43** (2023), 2084–2101. https://doi.org/10.12011/SETP2022-2158
8. T. H. Cui, J. S. Raju, Z. J. Zhang, Fairness and channel coordination, *Manage. Sci.,* **53** (2007), 1303–1314. https://doi.org/10.1287/mnsc.1060.0697
9. Y. Zhou, X. Ye, Differential game model of joint emission reduction strategies and contract design in a dual-channel supply chain, *J. Clean. Prod.,* **190** (2018), 592–607. https://doi.org/10.1016/j.jclepro.2018.04.133
10. Q. Wang, D. Zhao, Cooperative strategy of carbon emissions reduction and promotion in a two-echelon supply chain, *Control Decis.,* **29** (2014), 307–314.
11. X. Peng, Y. Tao, C. Wang, Z. Zhong, Research on low-carbon supply chain decision-making under carbon cap-and-trade and subsidy policy, *Int. J. Low-Carbon Technol.,* **17** (2022), 1061–1074. https://doi.org/10.1093/ijlct/ctac086
12. F. Ren, B. Hu, Decisions and coordination in low-carbon supply chains with a wholesale price constraint under government subsidies, *Int. J. Prod. Econ.,* **277** (2024), 109407. https://doi.org/10.1016/j.ijpe.2024.109407
13. G. Yan, Y. Ni, Pricing and low-carbon decisions in an uncertain supply chain with cap-and-trade regulation, *J. Intell. Fuzzy Syst.,* **46** (2024), 2877–2897. https://doi.org/10.3233/JIFS-232607
14. Q. Lin, H. Liao, Y. Liang, Research on the optimization of operational strategies for supply chain members under two carbon trading pathways in the context of carbon emission trade, *J. Ind. Manag. Optim.,* **21** (2025), 6384–6426. https://doi.org/10.3934/jimo.2025135
15. C. Zhu, J. Ma, J. Li, M. Goh, Grandfathering or benchmarking? The impact of carbon quota allocation rule on the joint emission reduction supply chain, *Int. J. Prod. Res.,* **63** (2025), 3608–3629. https://doi.org/10.1080/00207543.2024.2425777
16. S. Wang, L. Liu, J. Wen, Product pricing, green effort decisions and coordination in a dynamic three-echelon green supply chain, *J. Ind. Manag. Optim.,* **20** (2024), 2906–2933. https://doi.org/10.3934/jimo.2024033

17. Z. Zhang, L. Yu, Dynamic optimization and coordination of cooperative emission reduction in a dual-channel supply chain considering reference low-carbon effect and low-carbon goodwill, *Int. J. Environ. Res. Public Health,* **18** (2021), 539. https://doi.org/10.3390/ijerph18020539

18. A. Wu, R. Zhang, Y. Sun, L. Sun, S. Wang, X. Wang, Differential games of supply chain on consideration of low-carbon reference effect under different carbon quota allocation methods, *Systems,* **12** (2024), 371. https://doi.org/10.3390/systems12090371

19. M. Gao, L. Xia, Q. Xiao, M. Goh, Incentive strategies for low-carbon supply chains with information updating of customer preferences, *J. Clean. Prod.,* **410** (2023), 137162. https://doi.org/10.1016/j.jclepro.2023.137162

20. C. Zhu, J. Ma, J. Li, M. Goh, Retailer alliance and power structure shift in green brand supply chain under low-carbon operating environment, *Int. J. Prod. Res.,* **64** (2026), 2753–2779. https://doi.org/10.1080/00207543.2025.2583474

21. E. Fehr, K. M. Schmidt, A theory of fairness, competition, and cooperation, *Q. J. Econ.,* **114** (1999), 817–868. https://doi.org/10.1162/003355399556151

22. G. E. Bolton, A. Ockenfels, ERC: A theory of equity, reciprocity, and competition, *Am. Econ. Rev.,* **90** (2000), 166–193. https://doi.org/10.1257/aer.90.1.166

23. O. Caliskan-Demirag, Y. F. Chen, J. Li, Channel coordination under fairness concerns and nonlinear demand, *Eur. J. Oper. Res.,* **207** (2010), 1321–1326. https://doi.org/10.1016/j.ejor.2010.07.017

24. T. H. Ho, X. Su, Y. Wu, Distributional and peer-induced fairness in supply chain contract design, *Prod. Oper. Manag.,* **23** (2014), 161–175. https://doi.org/10.1111/poms.12064

25. C. H. Loch, Y. Wu, Social preferences and supply chain performance: An experimental study, *Manage. Sci.,* **54** (2008), 1835–1849. https://doi.org/10.1287/mnsc.1080.0910

26. L. Chen, H. L. Lee, C. S. Tang, Supply chain fairness, *Prod. Oper. Manag.,* **31** (2022), 4304–4318. https://doi.org/10.1111/poms.13849

27. W. Jin, Q. Zhang, Decision making in trade credit financing: Impact of loss aversion and power imbalance, *Int. Trans. Oper. Res.,* **28** (2021), 2607–2632. https://doi.org/10.1111/itor.12912

28. W. Liu, S. Song, Y. Qiao, H. Zhao, Supply chain coordination with a loss-averse retailer and combined contract, *Mathematics,* **8** (2020), 586. https://doi.org/10.3390/math8040586

29. W. Xie, B. Chen, F. Huang, J. He, Coordination of a supply chain with a loss-averse retailer under supply uncertainty and marketing effort, *J. Ind. Manag. Optim.,* **17** (2021), 3393–3415. https://doi.org/10.3934/jimo.2020125

30. E. Katok, V. Pavlov, Fairness in supply chain contracts: A laboratory study, *J. Oper. Manag.,* **31** (2013), 129–137. https://doi.org/10.1016/j.jom.2013.01.001

31. F. Qin, F. Mai, M. J. Fry, A. S. Raturi, Supply-chain performance anomalies: Fairness concerns under private cost information, *Eur. J. Oper. Res.,* **252** (2016), 170–182. https://doi.org/10.1016/j.ejor.2016.01.033

32. V. Pavlov, E. Katok, W. Zhang, Optimal contract under asymmetric information about fairness, *Manuf. Serv. Oper. Manag.,* **24** (2021), 305–314. https://doi.org/10.1287/msom.2020.0945

33. Y. Zhou, M. Bao, X. Chen, X. Xu, Co-op advertising and emission reduction cost sharing contracts and coordination in low-carbon supply chain based on fairness concerns, *J. Clean. Prod.,* **133** (2016), 402–413. https://doi.org/10.1016/j.jclepro.2016.05.097

34. X. Qian, F. T. S. Chan, J. Zhang, M. Yin, Q. Zhang, Channel coordination of a two-echelon sustainable supply chain with a fair-minded retailer under cap-and-trade regulation, *J. Clean. Prod.,* **244** (2020), 118715. https://doi.org/10.1016/j.jclepro.2019.118715

35. L. Xia, T. Guo, J. Qin, X. Yue, N. Zhu, Carbon emission reduction and pricing policies of a supply chain considering reciprocal preferences in cap-and-trade system, *Ann. Oper. Res.,* **268** (2018), 149–175. https://doi.org/10.1007/s10479-017-2657-2

36. Y. Zhang, Y. Yi, Sustainable production strategies of loss-averse competitive manufacturers with reference dependence under cap-and-trade policy, *Transp. Res. Part E Logist. Transp. Rev.,* **192** (2024), 103809. https://doi.org/10.1016/j.tre.2024.103809

37. Z. Zhang, L. Yu, Joint emission reduction dynamic optimization and coordination in the supply chain considering fairness concern and reference low-carbon effect, *J. Ind. Manag. Optim.,* **18** (2022), 4201–4229. https://doi.org/10.3934/jimo.2021155

38. L. Xia, Y. Bai, S. Ghose, J. Qin, Differential game analysis of carbon emissions reduction and promotion in a sustainable supply chain considering social preferences, *Ann. Oper. Res.,* **310** (2022), 257–292. https://doi.org/10.1007/s10479-020-03838-8

39. C. Yu, Y. Zhang, L. Liu, T. W. Archibald, Low-carbon supply chain strategy and contract coordination considering manufacturers' fairness concerns, *Oper. Res.,* **24** (2024), 64. https://doi.org/10.1007/s12351-024-00869-y

40. P. Shi, K. Han, R. Hou, Co-op advertising and carbon emission reduction cost-sharing contracts in coordinating supply chain with reciprocal behavior under cap-and-trade regulation, *J. Manag. Sci. China,* **27** (2024), 57–81. https://doi.org/10.19920/j.cnki.jmsc.2024.12.004

41. D. Wu, H. Ding, W. Wang, Y. Cheng, Green technology investment and supply chain coordination strategies considering marketing efforts and risk aversion under carbon tax policy, *J. Ind. Manag. Optim.,* **21** (2025), 418–453. https://doi.org/10.3934/jimo.2024089

42. J. Chen, L. Sun, T. Zhang, R. Hou, Low carbon joint strategy and coordination for a dyadic supply chain with Nash bargaining fairness, *J. Ind. Manag. Optim.,* **19** (2023), 1282–1309. https://doi.org/10.3934/jimo.2021229

43. B. Beyer, R. Chaskel, S. Euler, J. Gassen, A. K. Großkopf, T. Sellhorn, How does carbon footprint information affect consumer choice? A field experiment, *J. Account. Res.,* **62** (2024), 101–136. https://doi.org/10.1111/1475-679X.12505



AIMS Press

© 2026 the Author(s), licensee AIMS Press. This is an open access article distributed under the terms of the Creative Commons Attribution License (https://creativecommons.org/licenses/by/4.0)